Essentials of Photon Echoes: Mid-IR Photon Echo Spectroscopy on HOD/D_2O as Example

• E.T.J. Nibbering

Max Born Institut für Nichtlineare Optik und Kurzzeitspektroskopie
Berlin-Adlershof, Germany

SFB-450 Analyse und Steuerung ultraschneller
photoinduzierter Reaktionen
Teilprojekt B2

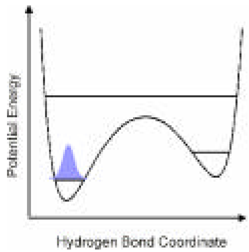

Outline

- Hydrogen bonding: HOD in D_2O
- Bloch vs. Kubo models
- Two pulse photon echoes: dephasing
- Three pulse photon echoes
  - Population relaxation and spectral diffusion
  - Three pulse echo peak shift measurements (3PEPS)

Hydrogen Bonds in Water and Ice

O-H···O

hydrogen bonds between water molecules determine the structure and other physical properties

Water: unordered liquid structure

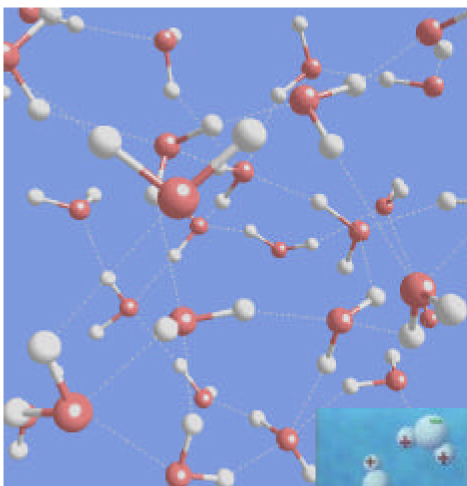

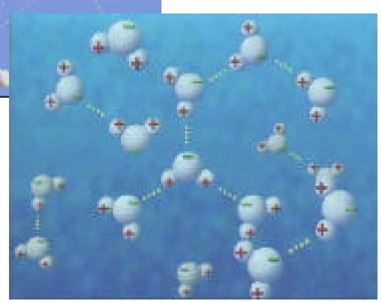

binding energy
10.7 kJ/mol

Ice: ordered crystal structure

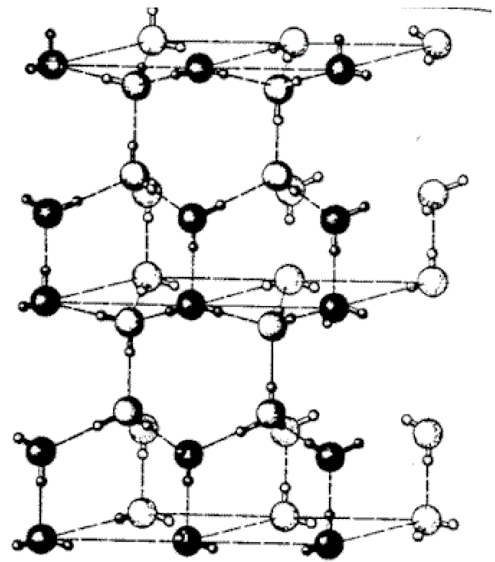

Hydrogen Bonding and IR Spectroscopy

Hadži and Bratos (1976): absorption line positions and shapes

Weak Intermolecular H-Bond

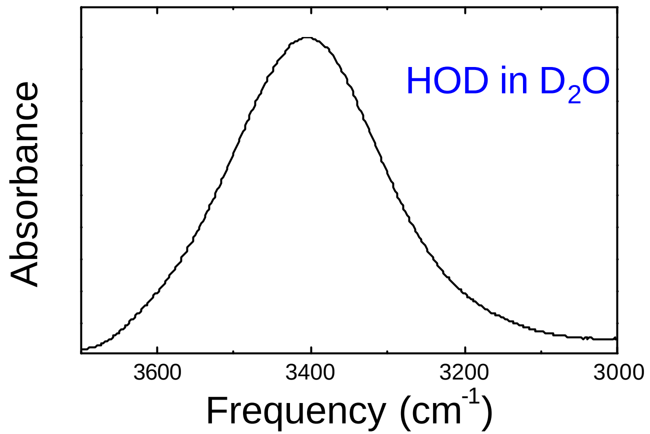

S. Bratos, J.-Cl. Leicknam, G. Gallot, H. Ratajczak, In *Ultrafast hydrogen bonding dynamics and proton transfer processes in the condensed phase*, T. Elsaesser and H. J. Bakker, Eds. (Kluwer, Dordrecht, 2002), pp. 5-30.

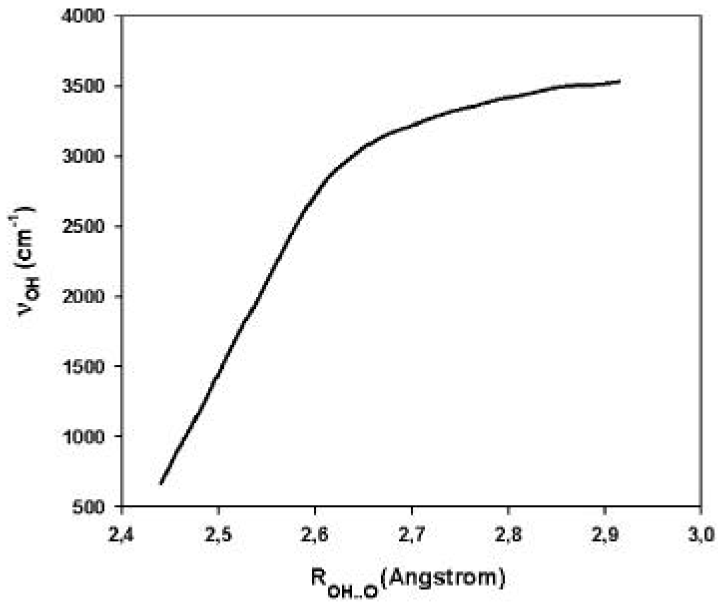

O-H/O-D stretching band

- Red-shift of ν(X-H)
  reduced force constant
- Very strong broadening
  distribution of bond lengths (& angles!)
  anharmonic coupling to low-frequency modes
  homogeneous broadening

Time Scales of Molecular Relaxation Phenomena

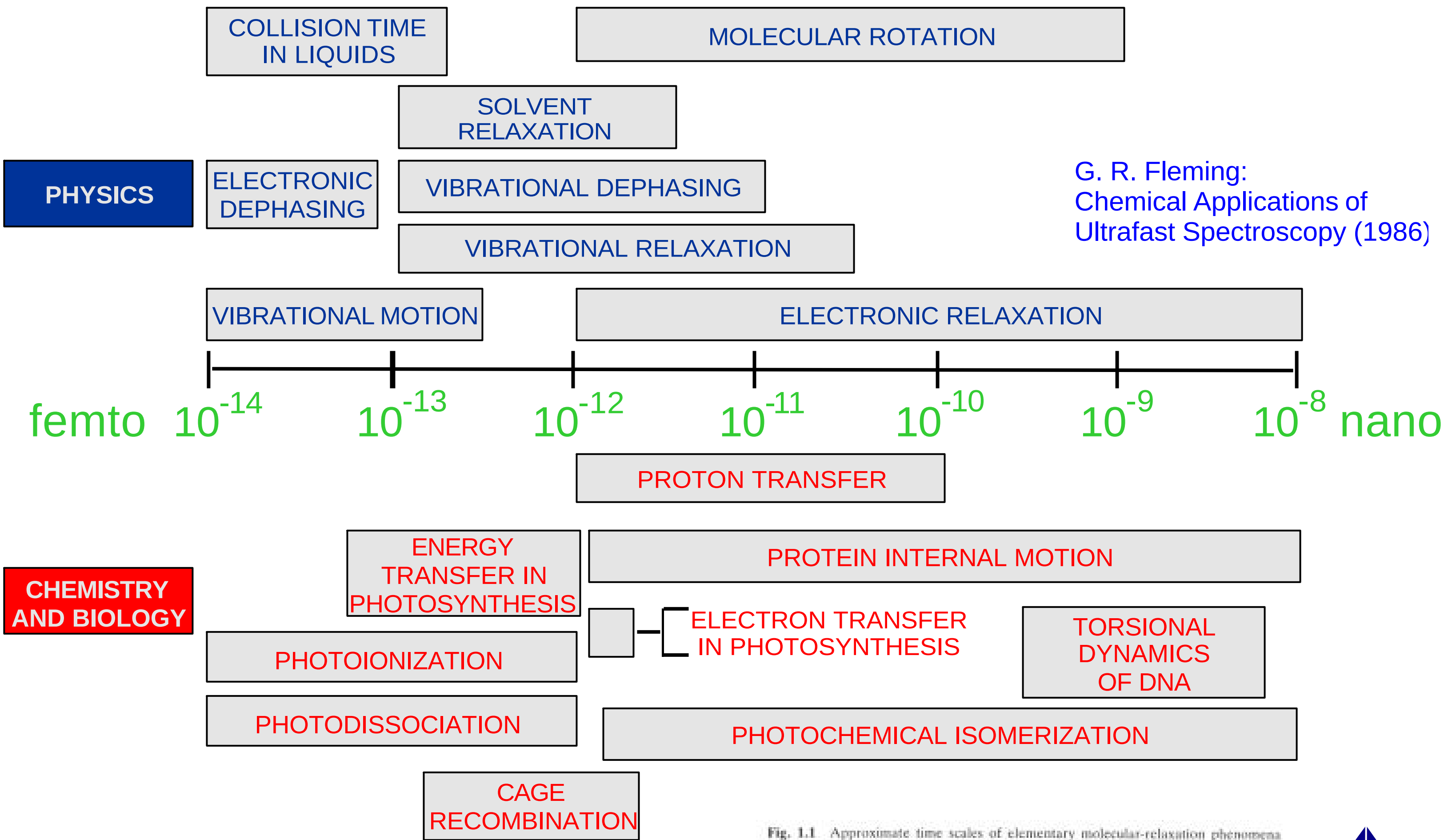

G. R. Fleming:
Chemical Applications of
Ultrafast Spectroscopy (1986)

Fig. 1.1 Approximate time scales of elementary molecular-relaxation phenomena and of some chemical and biological manifestations of these phenomena. The extent of the presented time range (10^{-14} to 10^{-8} s) is not intended to imply upper or lower limits on some of the processes

Femtosecond Mid-IR Photon Echo Spectroscopy

E.L. Hahn 1950: Spin Echo

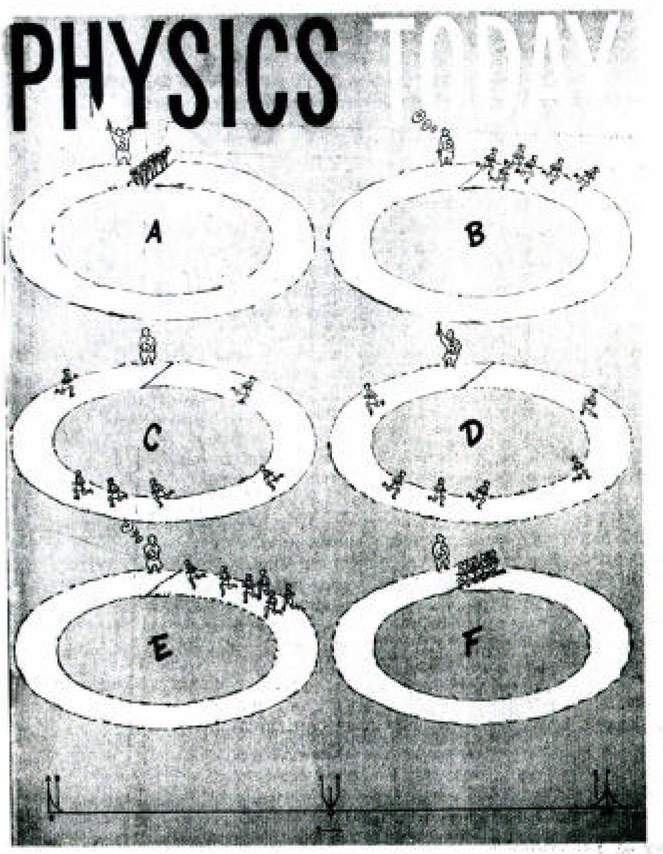

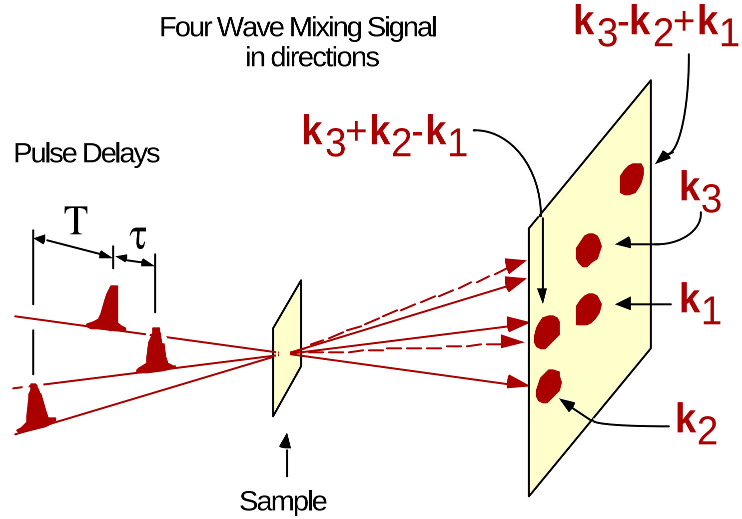

- Transient Grating Scattering: $\tau = 0$; scan T.
- 2 Pulse Photon Echo: T = 0; scan τ.
- 3 Pulse Photon Echo: scan τ; scan T.
- Echo Peak Shift Measurement:
  determine $\tau_{max}(T)$ where $\partial S_{3PE}/\partial\tau = 0$

Independent Two-Level Systems: Bloch Model

Transition coupled to solvent bath with infinitely short or infinitely long correlation time (Bloch model)

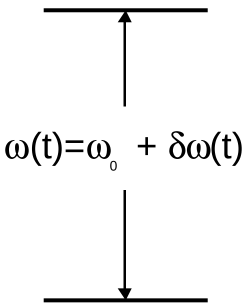

Response described by frequency fluctuation correlation function

$\langle\delta\omega(t)\delta\omega(0)\rangle=\pi\,\Gamma_{hom}\,\delta(t) + (\Delta_{ih})^2$

Γ_{hom} : homogeneous broadening amplitude
Δ_{ih}: inhomogeneous broadening amplitude

Homogeneous line width: $G_{hom}=1/pT_2$
with: $1/T_2=1/(T_2^*)+1/(2T_1)$

T_2 : dephasing time, T_2*: pure dephasing time,

T_1: population relaxation time

Frequency fluctuation correlation function with infinite short & infinitely long components

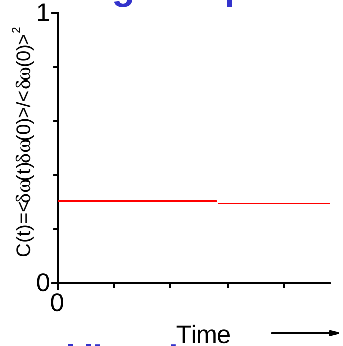

Spectral line shape convolution of Gaussian inhomogeneous and Lorentzian homogeneous broadening contributions (Voigt profile)

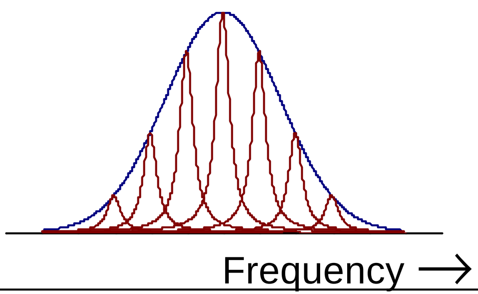

Independent Two-Level Systems: Kubo Model

Transition coupled to solvent bath with finite correlation time (Kubo model)

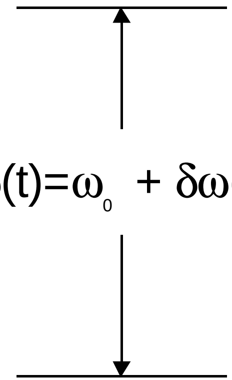

$$\omega(t)=\omega_0 + \delta\omega(t)$$

Response described by frequency fluctuation correlation function

$\langle\delta\omega(t)\delta\omega(0)\rangle=(\Delta_h)^2\exp(-t/\tau_c)$

Δ_h : fluctuation amplitude
τ_c: correlation time

- $\Delta_h \tau_c \ll 1$: fast modulation limit $T_2^*=[(\Delta_h)^2 \tau_c]^{-1}$
- $\Delta_h \tau_c \gg 1$: static limit

Frequency fluctuation correlation function with finite decay time

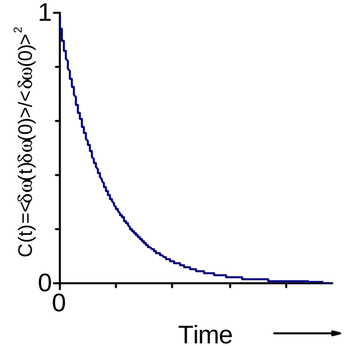

Spectral line shape interpolates between Gaussian and Lorentzian limits

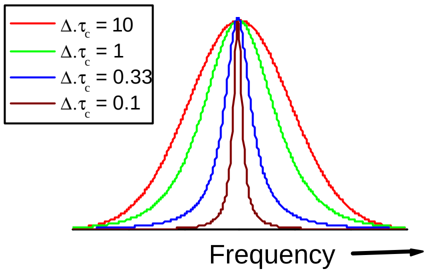

2PE Double-Sided Feynman Diagrams: 2-Level System

$$P^{(3)}(t) = \int\int\int R_a(t_3,t_2,t_1)E_i(t-t_3-t_i)E_j(t-t_3-t_2-t_j)E_k(t-t_3-t_2-t_1-t_k)e^{i\omega_i(t-t_3-t_i)+i\omega_j(t-t_3-t_2-t_j)+i\omega_k(t-t_3-t_2-t_1-t_k)}dt_1dt_2dt_3$$

a: index of double-sided Feynman diagrams

i,j,k: index of applied light field(s) with delays $t_{i,j,k}$

field interaction order:

δ-pulse: $E_i(\tau)=E\delta(\tau-\tau_i)$

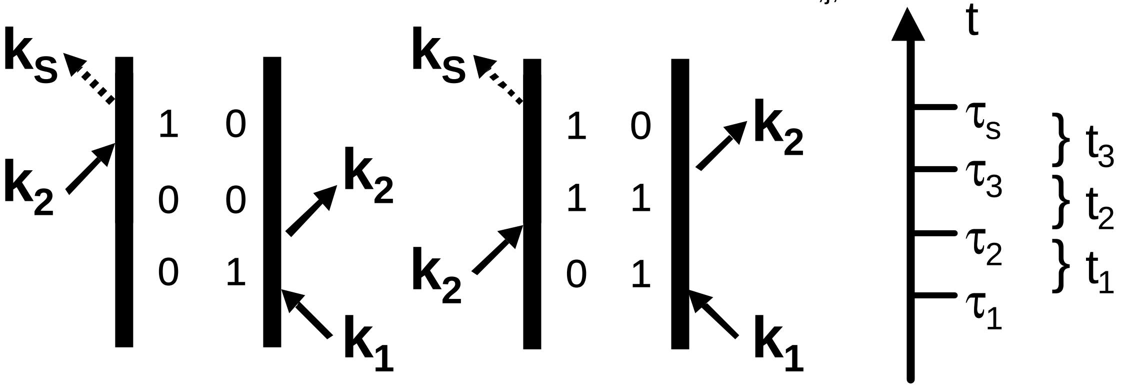

$E_2(t-t_3-\tau)$

$E_2(t-t_3-t_2-\tau)$

$E_1^*(t-t_3-t_2-t_1)$

$t-t_3 = t'$

$t_2 = 0$

$t_1 = \tau$

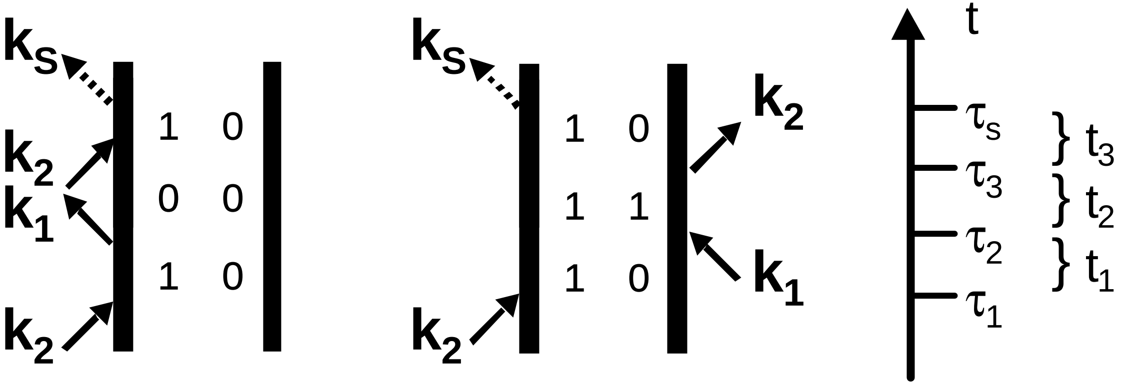

only $\tau=0$

$E_2(t-t_3-\tau)$

$E_1^*(t-t_3-t_2)$

$E_2\ (t-t_3-t_2-t_1-\tau)$

$t_3 = t$

$t_2 = 0$

$t_1 = 0$

Rephasing vs. Non-Rephasing Feynman Diagrams

$$P^{(3)}(t)= \int\int\int R_a(t_3,t_2,t_1)E_i(t-t_3-t_i)E_j(t-t_3-t_2-t_j)E_k(t-t_3-t_2-t_1-t_k)e^{i\omega_i(t-t_3-t_i)+i\omega_j(t-t_3-t_2-t_j)+i\omega_k(t-t_3-t_2-t_1-t_k)}dt_1dt_2dt_3$$

a: index of double-sided Feynman diagrams

i,j,k: index of applied light field(s) with delays $t_{i,j,k}$

contribution in $R_a(t_3,t_2,t_1)$

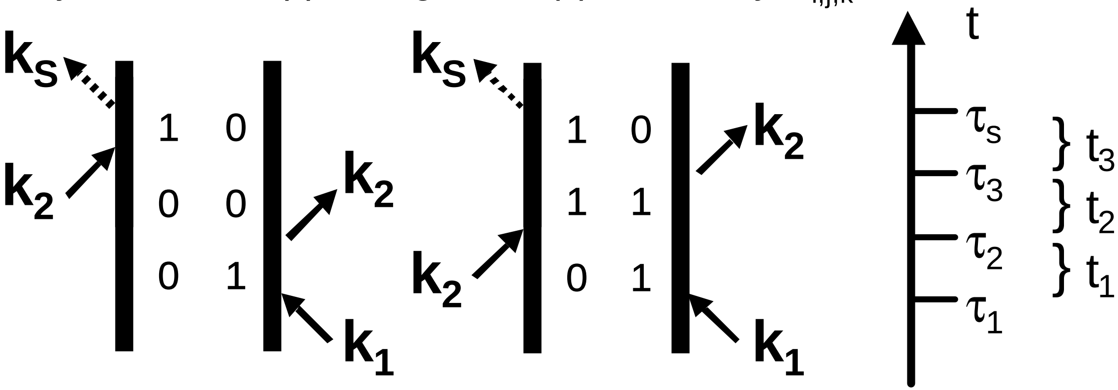

$e^{-i\omega_{10}t_3-t_3/T_2}$

$e^{-i\omega_{01}t_1-t_1/T_2}$

"rephasing" → echo

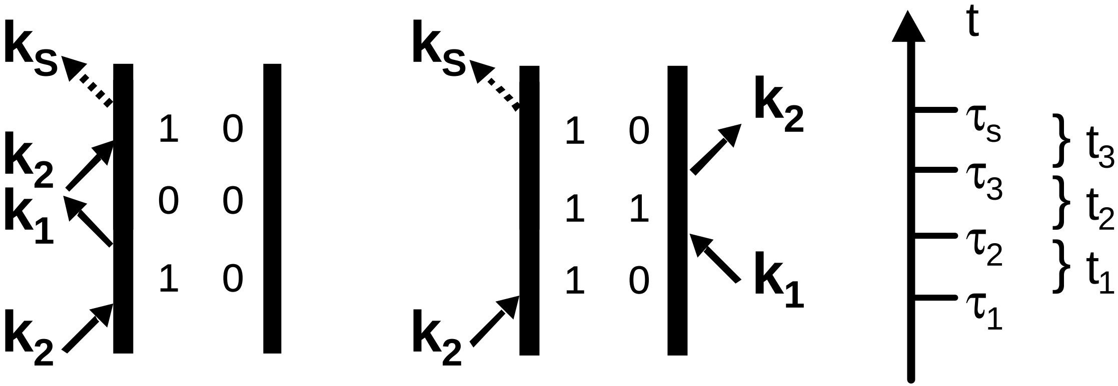

$e^{-i\omega_{10}t_3-t_3/T_2}$

$e^{-i\omega_{10}t_1-t_1/T_2}$

"non-rephasing" → virtual echo

Rephasing in Echo Experiment I

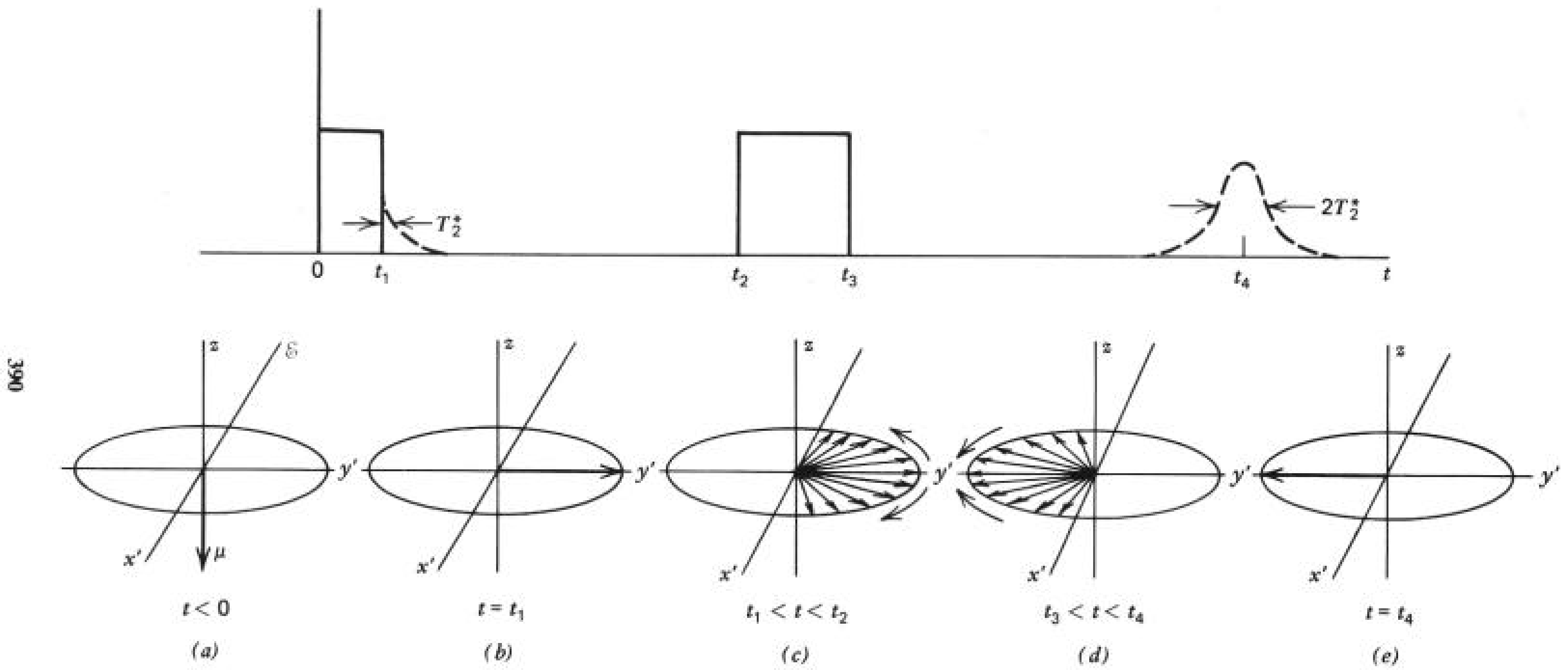

Fig. 21.7 Schematic drawings describing the echo phenomenon. The upper picture shows the pulse excitation sequence. The lower picture depicts the precession of the pseudo-dipoles in the rotating frame at various times.

Y.R. Shen, The Principles of Nonlinear Optics

Rephasing in Echo Experiment II

E.L. Hahn 1950:
Spin Echo

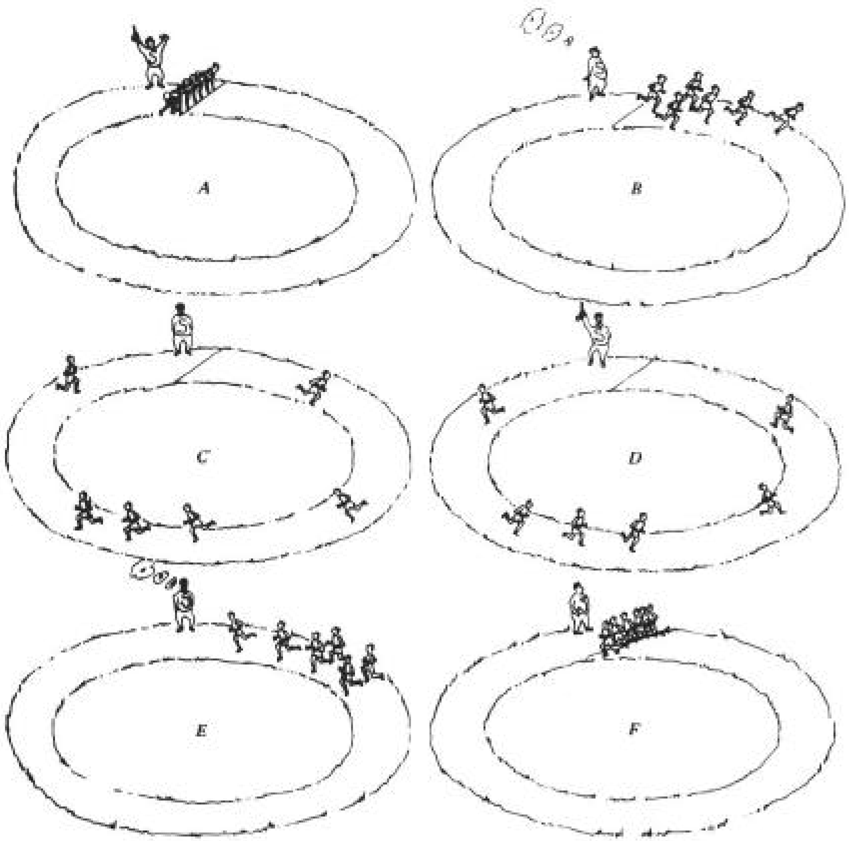

Fig. 9.2 Dephasing and reversal on a race track, leading to coherent rephasing and an "echo" of the starting configuration. [From *Phys. Today*, front cover, November 1953. Reproduced by permission.]

Chirped Four Wave Mixing

Comparison of relative contributions of rephasing and non-rephasing diagrams

K. Duppen, F. de Haan, E. T. J. Nibbering, and D. A. Wiersma
Phys. Rev. A **47**, 5120-5137 (1993)

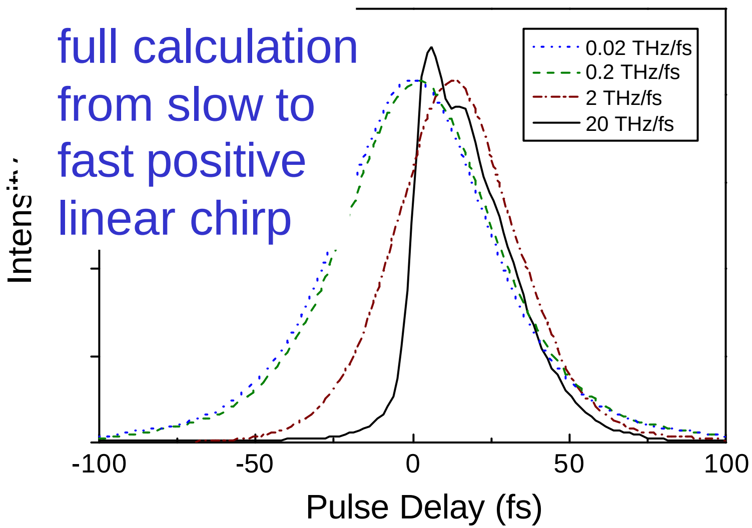

FIG. 5. Delay dependence of the time-integrated signal intensity for four different chirp rates of the optical fields. The chirp rates b are 0.02 THz/fs (dotted curve), 0.2 THz/fs (dashed curve), 2 THz/fs (dot-dashed curve), and 20 THz/fs (solid curve). The system dynamics is as in Fig. 4.

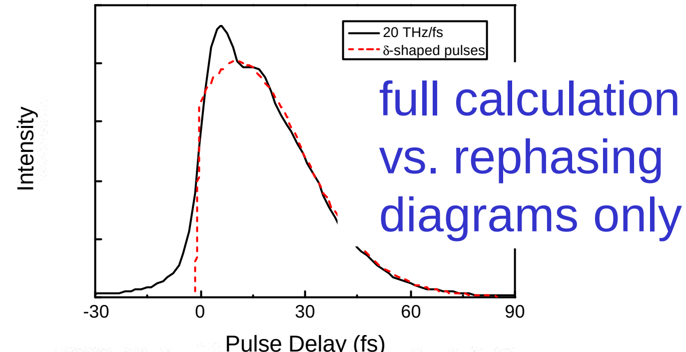

FIG. 6. Nonlinear signal expected for δ-shaped optical pulses (dashed line) and for chirped excitation (solid line). The chirp rate is fast compared to the system dynamics: $b = 20$ THz/fs. The system dynamics is as in Fig. 4.

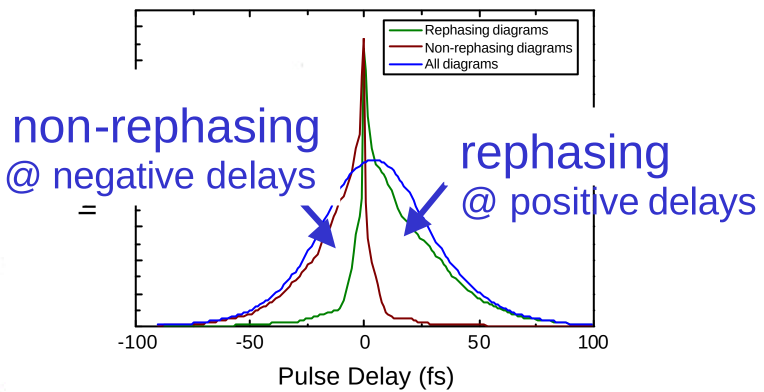

FIG. 7. Nonlinear chirped signal for pulses with a chirp rate $b = 0.5$ THz/fs (solid line). When only diagrams I and II of Fig. 3 are used in the calculation, the dotted line results. Diagrams III and IV of Fig. 3 lead to a signal trace given by the dashed line. The infinities at delay $\tau = 0$ fs cancel when the contributions from all diagrams are included in the calculation. The system dynamics is as in Fig. 4.

Electric Field Interactions Order

$$P^{(3)}(t)=\int\int\int R_a(t_3,t_2,t_1)E_i(t-t_3-t_i)E_j(t-t_3-t_2-t_j)E_k(t-t_3-t_2-t_1-t_k)e^{i\omega_i(t-t_3-t_i)+i\omega_j(t-t_3-t_2-t_j)+i\omega_k(t-t_3-t_2-t_1-t_k)}dt_1dt_2dt_3$$

a: index of double-sided Feynman diagrams

i,j,k: index of applied light field(s) with delays $t_{i,j,k}$

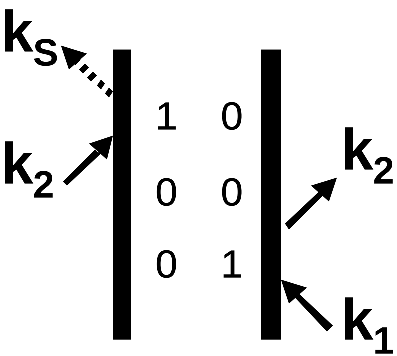

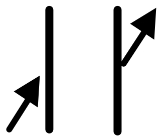

$E_i(t)e^{i\omega_i(t)}$

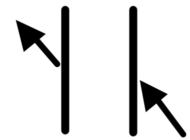

$E^*_i(t)e^{-i\omega_i(t)}$

$$E_2(t-t_3-\tau)E_2(t-t_3-t_2-\tau)E^*_1(t-t_3-t_2-t_1)e^{i\omega_2(t-t_3-\tau)+i\omega_2(t-t_3-t_2-\tau)-i\omega_1(t-t_3-t_2-t_1)}$$

Energy conservation: $\omega_s=\omega_3+\omega_2-\omega_1=2\omega_2-\omega_1$

Phase matching: $\mathbf{k}_s=\mathbf{k}_3+\mathbf{k}_2-\mathbf{k}_1=2\mathbf{k}_2-\mathbf{k}_1$

$$R_a(t_3,t_2,t_1)=(-i)^l(i)^r\,|\mu_{10}|^4\,e^{-i\omega_{10}(t_3-t_1)}\,e^{-g(t_1)+g(t_2)-g(t_3)-g(t_2+t_1)-g(t_3+t_2)+g(t_3+t_2+t_1)}$$

l=number of interactions on the left

r=number of interactions on the right

Line shape function $g(t)=\int_0^t\int_0^{\tau_2}C(\tau_2-\tau_1)\,d\tau_2 d\tau_1$

Polarisation in Bloch & Kubo Cases

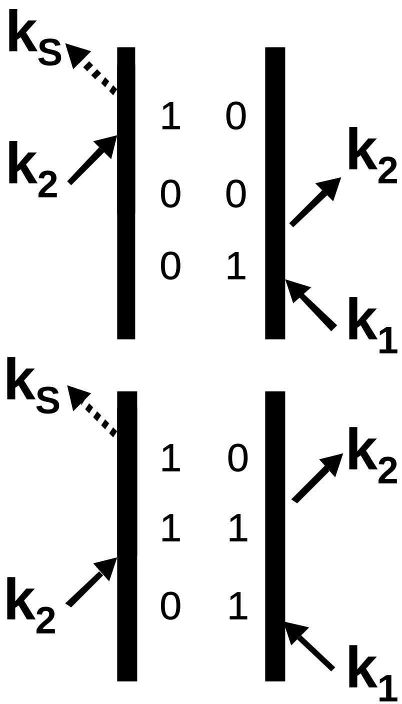

These 2 diagrams lead to same expressions in the case of two pulse photon echo

δ-pulse:
$E_i(\tau)=E\delta(\tau-\tau_i)$

$t-t_3 = t'$ $\quad t_2 = 0$ $\quad t_1 = \tau$ $\quad \omega_2=\omega_1=\omega_{10}$

$E_2E_2E^*_1 e^{i\,(2\omega_2-\omega_1)\,(t'-\tau)}$

$R_a(t',0,\tau)= (-i)^2(i)^2\,|\mu_{10}|^4\, e^{-i\omega_{10}(t'-\tau)}\, e^{-2g(\tau) - 2g(t') + g(t'+\tau)}$

$I^{2PE}(\tau) = \int |P^{(3)}(t',\tau)|^2 dt' = 4(E_2E_2E^*_1)^2|\mu_{10}|^8\, e^{-4g(\tau) - 4g(t') + 2g(t'+\tau)}$

scales as E^6

scales as $|\mu_{10}|^8$

Bloch limit: $g(t) = [1/T_2]\,t + [(\Delta_{ih})^2/2]\,t^2$

Kubo case: $g(t) = [(\Delta_{ih})^2\,\tau_c^2]\,\{e^{-t/\tau_c} + t/\tau_c - 1\}$

Bloch Limit: 2PE Experiment

A $\langle \delta\omega(t)\delta\omega(0) \rangle = \delta(t)/T_2$ $I^{2PE}(t',\tau) \propto \exp(-2\tau/T_2 - 2t'/T_2)$ $I^{2PE}(\tau) \propto \exp(-2\tau/T_2)$

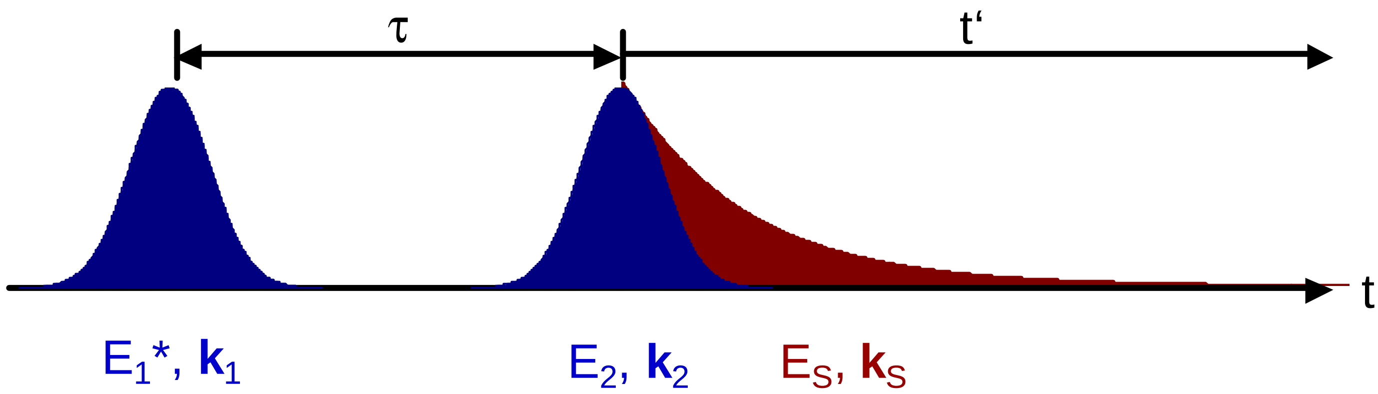

B $\langle \delta\omega(t)\delta\omega(0) \rangle = \delta(t)/T_2 + (\Delta_{ih})^2$ $I^{2PE}(t',\tau) \propto \exp(-2\tau/T_2 - 2t'/T_2 - (\Delta_{ih})^2 (t'-\tau)^2)$ $I^{2PE}(\tau) \propto \exp(-4\tau/T_2)$

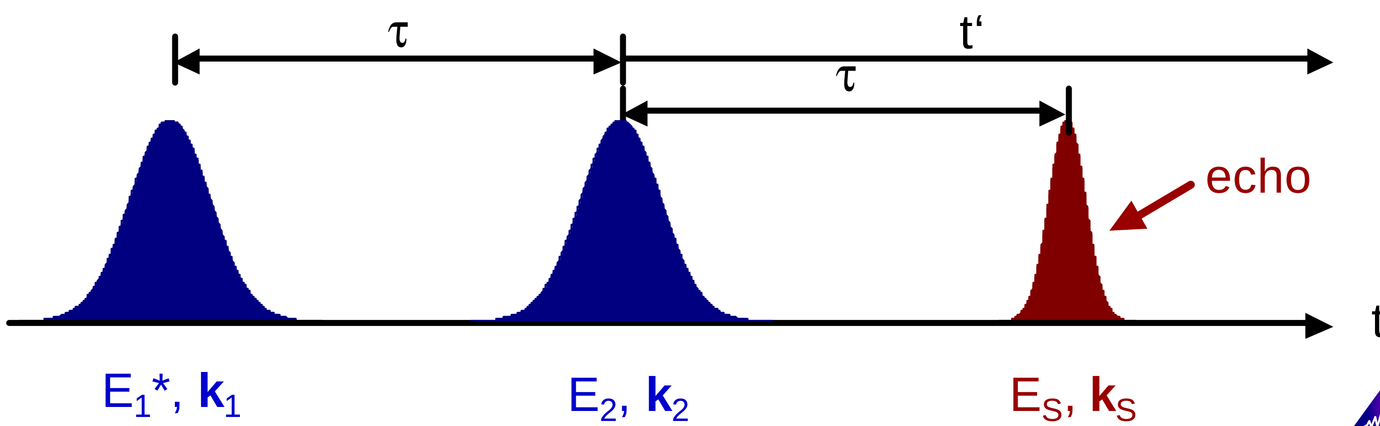

Independent Two-Level Systems: Bloch Model

Homogeneous line width

$G_{hom}=1/pT_2$ $\quad$ $1/T_2=1/(T_2^*)+1/(2T_1)$

T_2 : dephasing time, T_2^*: pure dephasing time,
T_1: population relaxation time

2-pulse photon echo (2-PE) (T=0,scan t)

Signals in directions $2\mathbf{k}_2-\mathbf{k}_1$, $\mathbf{2k}_1-\mathbf{k}_2$

$I^{2PE}(\omega,t',T=0,\tau) \propto |P^{(3)}(\omega,t',T=0,\tau)|^2$

Spectral line shape convolution of Gaussian inhomogeneous and Lorentzian homogeneous broadening contributions (Voigt profile)

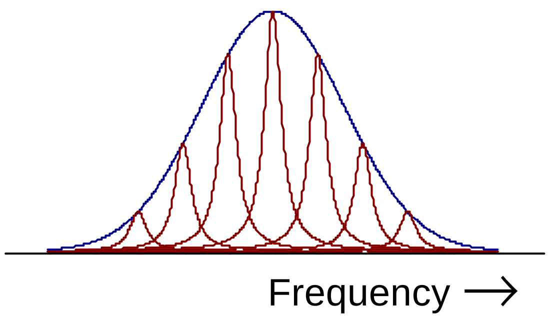

Time evolution of 2-PE signals

Independent 2-level systems

- Homogeneous broadening

  $I^{2PE}(\Delta t_{12}=\tau) \propto \exp(-2\tau/T_2)$

  (free induction decay)

- Dominant inhomogeneous broadening

  $I^{2PE}(\Delta t_{12}=\tau) \propto \exp(-4\tau/T_2)$
  (photon echo)

Kubo Case: 2PE Experiment

Echo maximum does not exceed τ_c (frequency fluctuation correlation time)

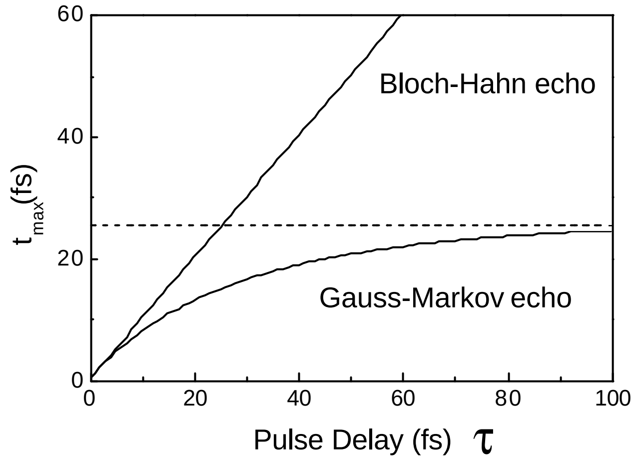

fig. 6.7 *Time at which the maximum of the signal amplitude occurs for a conventional (Bloch-Hahn) echo and an echo with (Gaussian-Markovian) stochastic system modulations.*

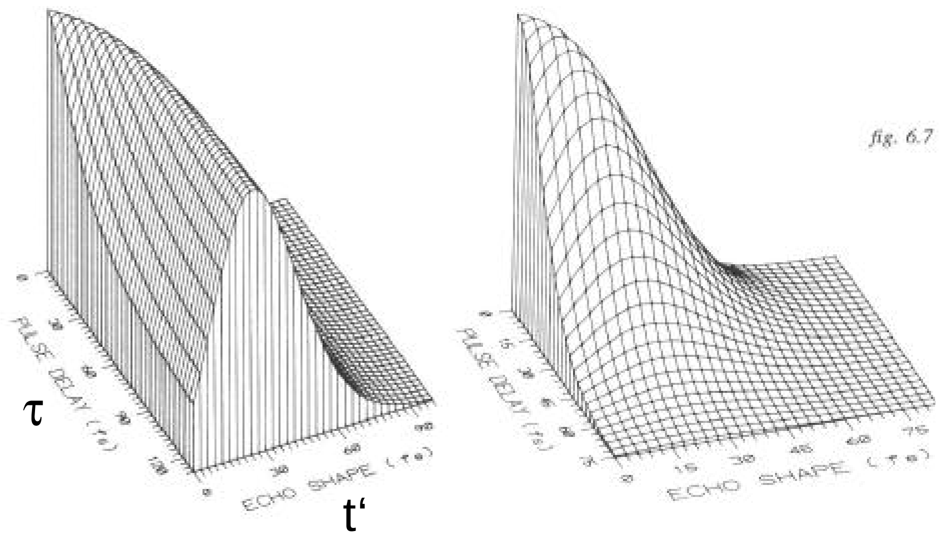

fig. 6.6 *The normalized photon echo profile is shown on the left and the tw dimensional relaxation function $R_{LII}(t, \tau)$ is displayed on the right. For boi plots the parameter values of fig. 6.5 were used.*

E.T.J. Nibbering, thesis
“Femtosecond optical dynamics in liquids”

Independent Two-Level Systems: Kubo Model

Transition coupled to solvent bath with finite correlation time (Kubo model)

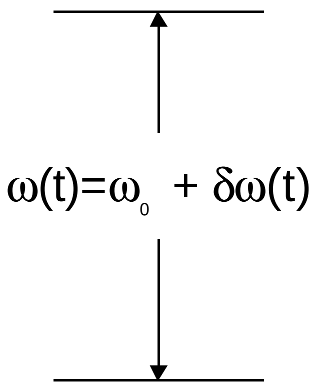

Response described by frequency fluctuation correlation function

$\langle \delta\omega(t)\delta\omega(0)\rangle = (\Delta_h)^2 \exp(-t/\tau_c)$

Δ_h : fluctuation amplitude
τ_c: correlation time

- $\Delta_h \tau_c << 1$: fast modulation limit $T_2^* = [(\Delta_h)^2 \tau_c]^{-1}$
- $\Delta_h \tau_c >> 1$: static limit

Spectral line shape interpolates between Gaussian and Lorentzian limits

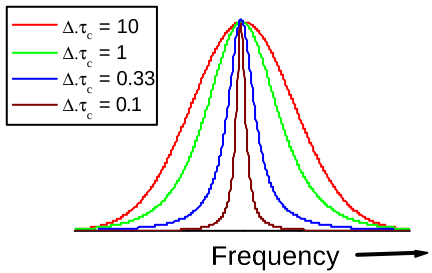

2PE-signal interpolates between Gaussian and exponential decay

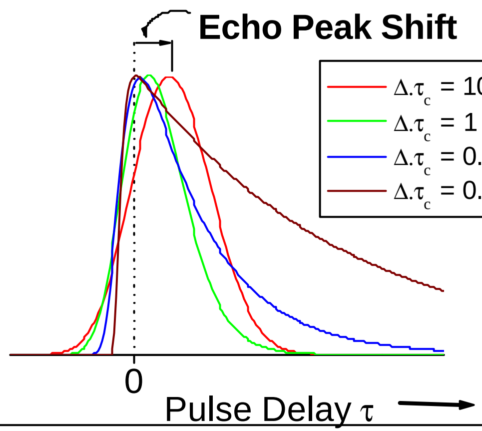

Vibrations: 3-Level System

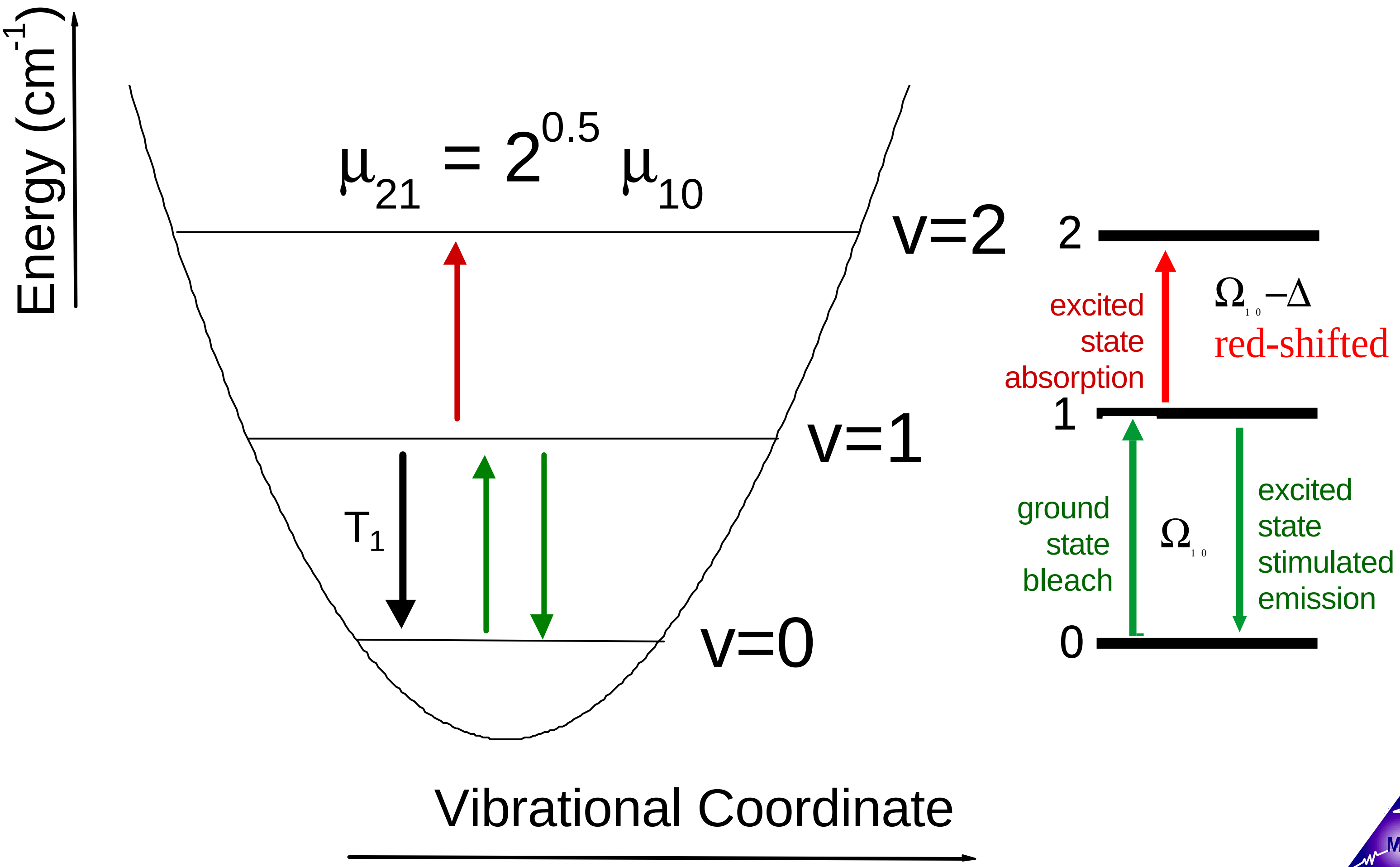

2PE Double-Sided Feynman Diagrams: 3-Level System

$$P^{(3)}(t) = \int\int\int R_a(t_3,t_2,t_1)E_i(t-t_3-t_i)E_j(t-t_3-t_2-t_j)E_k(t-t_3-t_2-t_1-t_k)e^{i\omega_i(t-t_3-t_i)+i\omega_j(t-t_3-t_2-t_j)+i\omega_k(t-t_3-t_2-t_1-t_k)}dt_1dt_2dt_3$$

a: index of double-sided Feynman diagrams

i,j,k: index of applied light field(s) with delays $t_{i,j,k}$

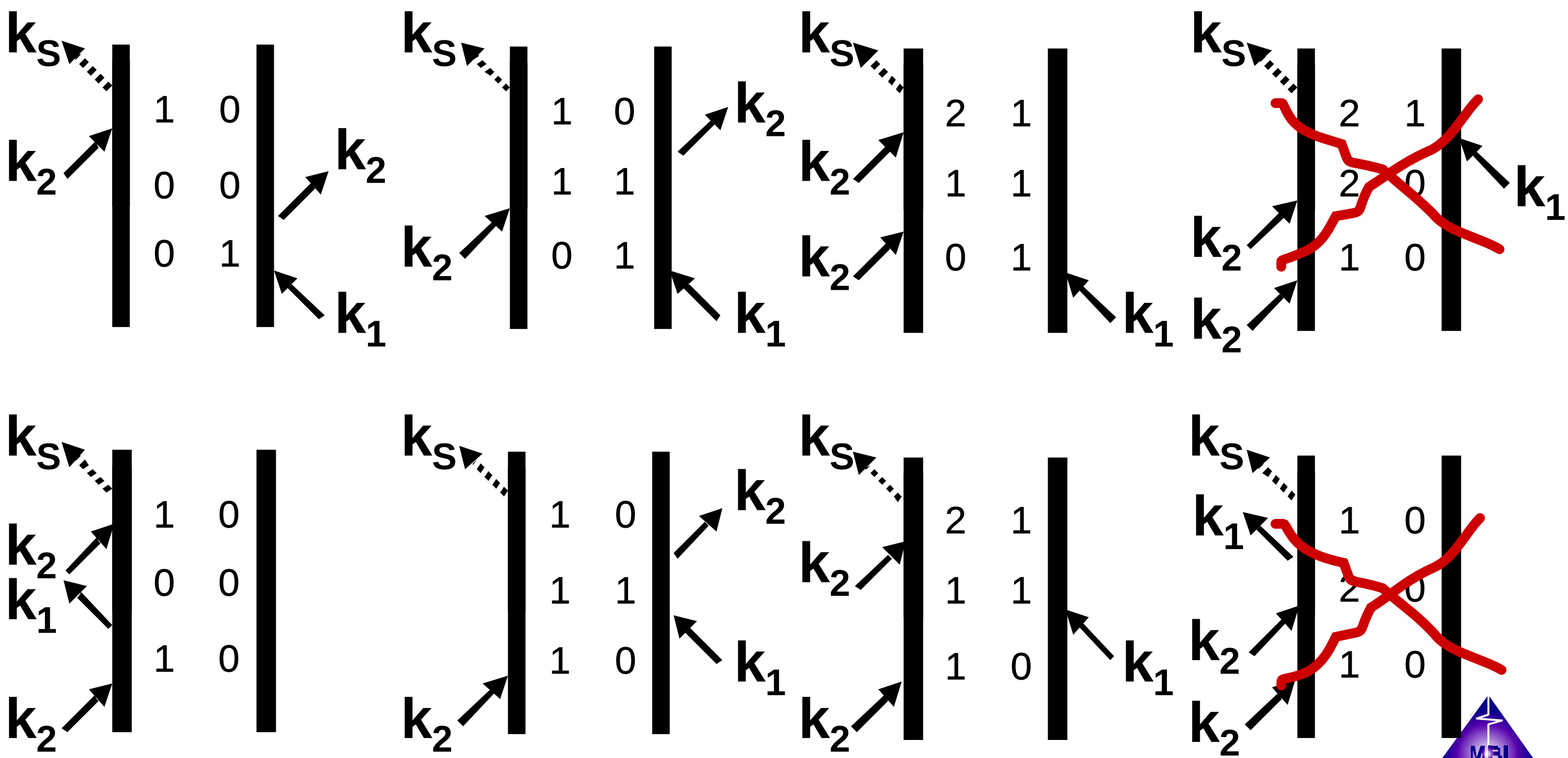

Two Pulse Photon Echo Study of HOD in D_2O

O-H stretching band and laser spectra

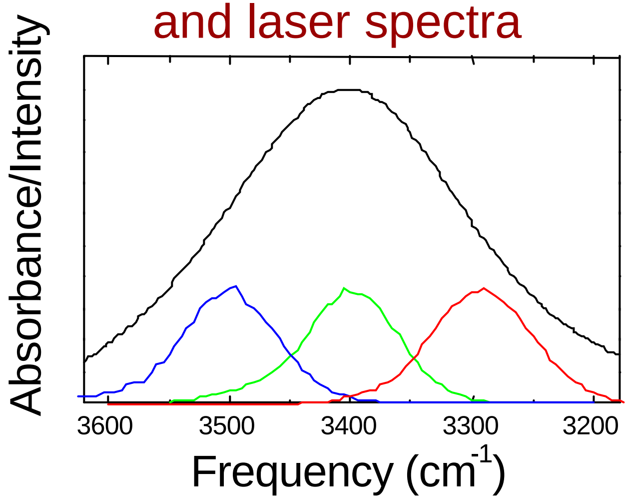

Two pulse photon echo results show coherence decay ~ 30 fs

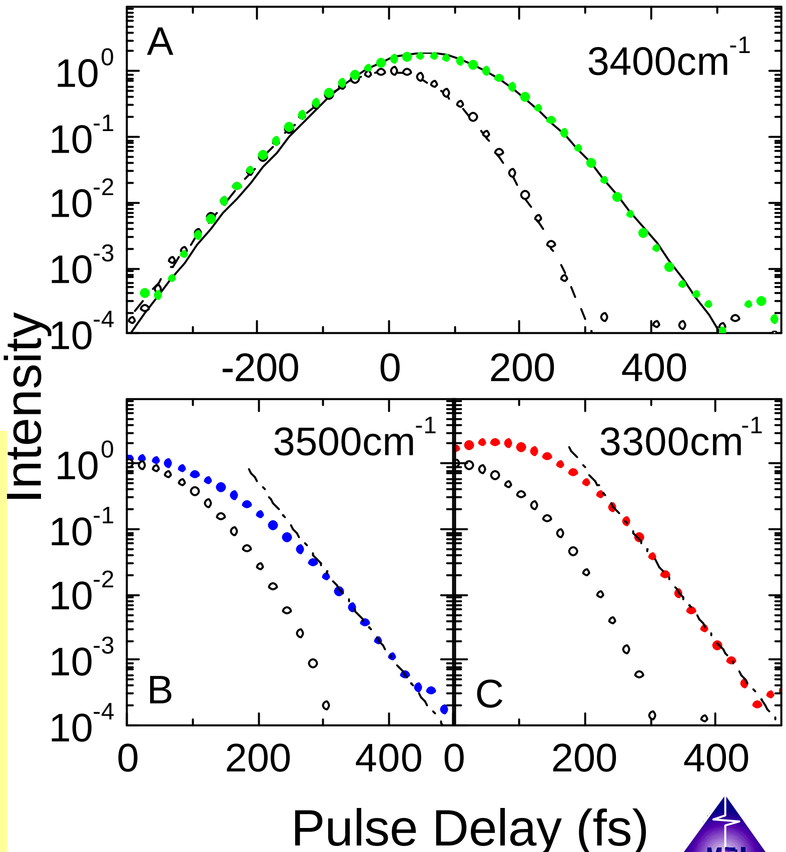

Fast component in dephasing dynamics of O-H stretching mode in HOD

- Very fast vibrational dephasing
- Pure dephasing time T_2^*=90 fs
- Γ_{hom} = 120 cm^{-1} ($T_1 \approx 1$ps)

J. Stenger *et al*., Phys. Rev. Lett. **87**, 027401 (2001)

3PE Double-Sided Feynman Diagrams: 2-Level System

$$P^{(3)}(t)=\int\int\int R_a(t_3,t_2,t_1)E_i(t-t_3-t_i)E_j(t-t_3-t_2-t_j)E_k(t-t_3-t_2-t_1-t_k)e^{i\omega_i(t-t_3-t_i)+i\omega_j(t-t_3-t_2-t_j)+i\omega_k(t-t_3-t_2-t_1-t_k)}dt_1dt_2dt_3$$

a: index of double-sided Feynman diagrams

i,j,k: index of applied light field(s) with delays $t_{i,j,k}$

field interaction order:

δ-pulse: $E_i(\tau)=E\delta(\tau-\tau_i)$

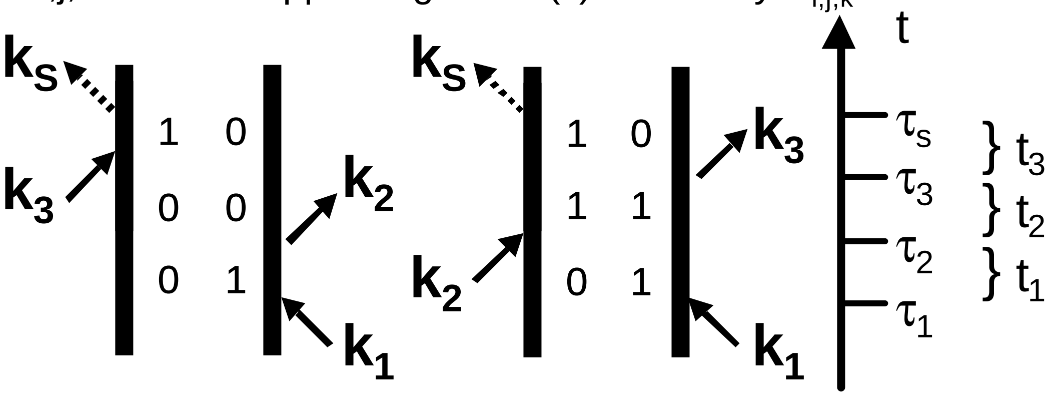

"rephasing" → echo

$E_3(t-t_3-\tau_{31})$

$E_2(t-t_3-t_2-\tau_{21})$

$E_1{}^*(t-t_3-t_2-t_1)$

$t-t_3 = t'$

$t_2 = \tau_{32} = T$

$t_1 = \tau_{21} = \tau$

$\tau_{32} = \tau_{31} - \tau_{21}$

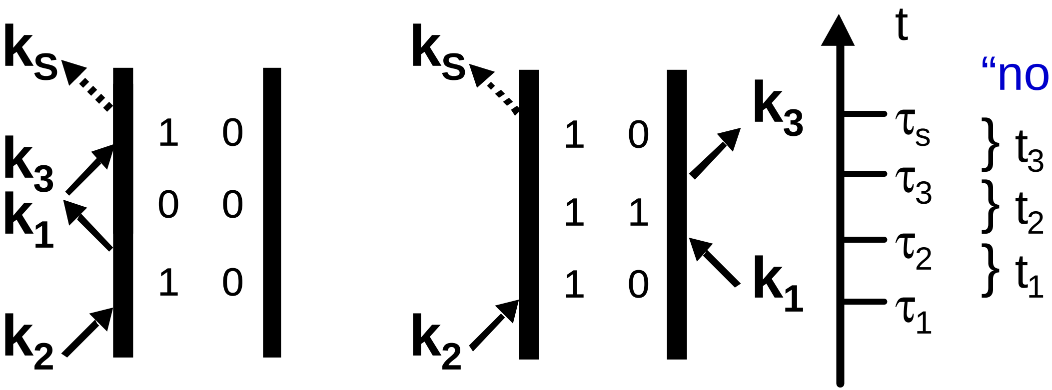

"non-rephasing" → virtual echo

$E_3(t-t_3-\tau_{31})$

$E_1{}^*(t-t_3-t_2)$

$E_2\ (t-t_3-t_2-t_1-\tau_{21})$

$t-t_3 = t'$

$t_2 = \tau_{31} = T$

$t_1 = \tau_{21} = \tau$

3PE Double-Sided Feynman Diagrams: 2-Level System

$$P^{(3)}(t) = \int\int\int R_a(t_3,t_2,t_1) E_i(t-t_3-t_i) E_j(t-t_3-t_2-t_j) E_k(t-t_3-t_2-t_1-t_k) e^{i\omega_i(t-t_3-t_i)+i\omega_j(t-t_3-t_2-t_j)+i\omega_k(t-t_3-t_2-t_1-t_k)} dt_1 dt_2 dt_3$$

a: index of double-sided Feynman diagrams

i,j,k: index of applied light field(s) with delays $t_{i,j,k}$

field interaction order:

δ-pulse: $E_i(\tau)=E\delta(\tau-\tau_i)$

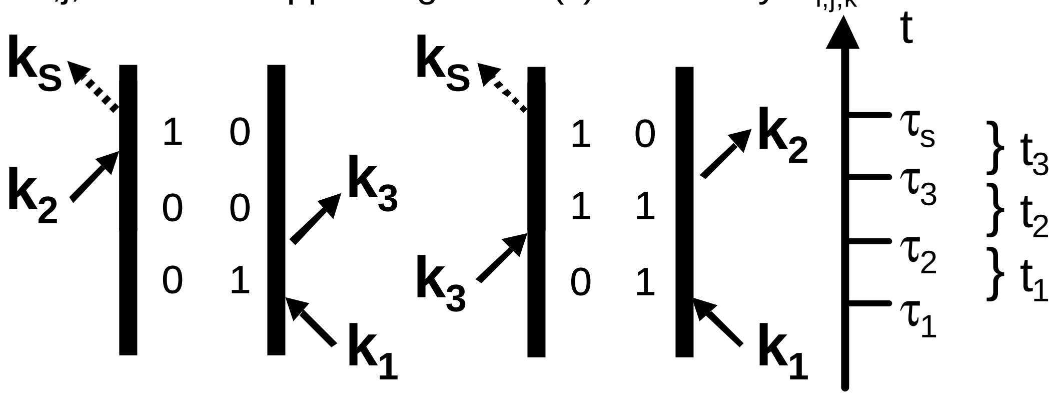

"rephasing" → echo

$E_2(t-t_3-\tau_{23})$

$E_3(t-t_3-t_2-\tau_{31})$

$E_1^*(t-t_3-t_2-t_1)$

$t-t_3 = t'$

$t_2 = \tau_{23} = T$

$t_1 = \tau_{31} = \tau$

$\tau_{23} = \tau_{21} - \tau_{31}$

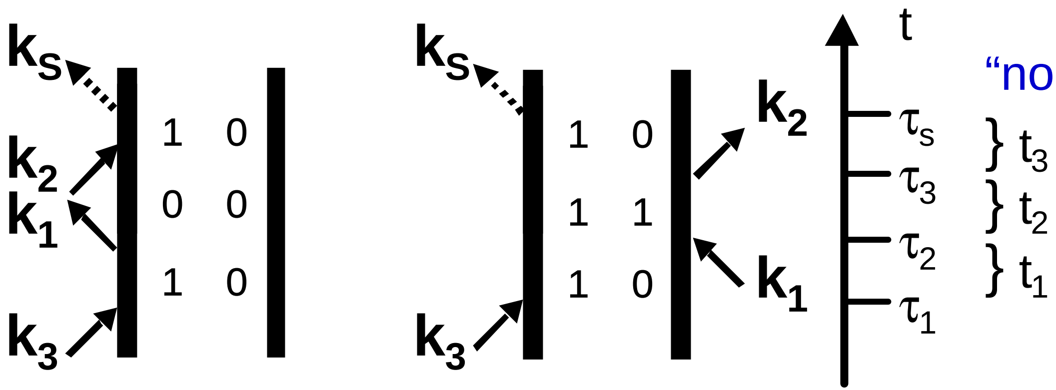

"non-rephasing" → virtual echo

$E_2(t-t_3-\tau_{21})$

$E_1^*(t-t_3-t_2)$

$E_3(t-t_3-t_2-t_1-\tau_{31})$

$t-t_3 = t'$

$t_2 = \tau_{21} = T$

$t_1 = \tau_{31} = \tau$

3PE: Population Relaxation

e^{-T/T_1} $\qquad$ e^{-T/T_1}

δ-pulse: $E_i(\tau)=E\delta(\tau-\tau_i)$

contribution in $R_a(t_3,t_2,t_1)$

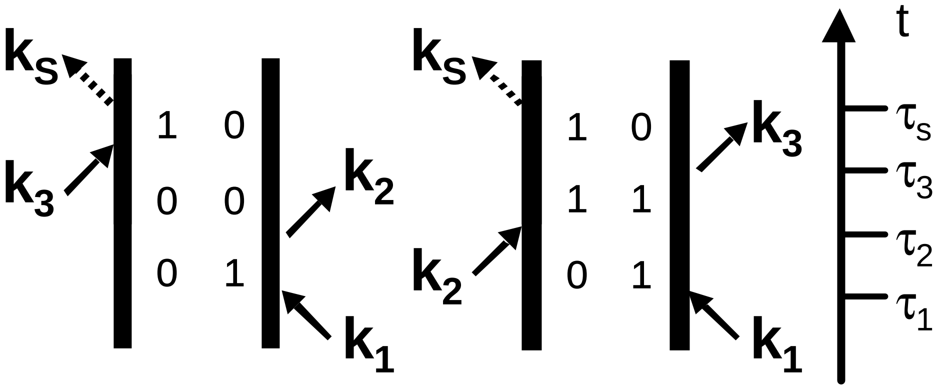

"rephasing" → echo

} $t-t_3=t'$ $\qquad$ $e^{-i\omega_{10}t'-t'/T_2}$

} $t_2=\tau_{32}=T$ $\qquad$ e^{-T/T_1}

} $t_1=\tau_{21}=\tau$ $\qquad$ $e^{-i\omega_{01}\tau-\tau/T_2}$

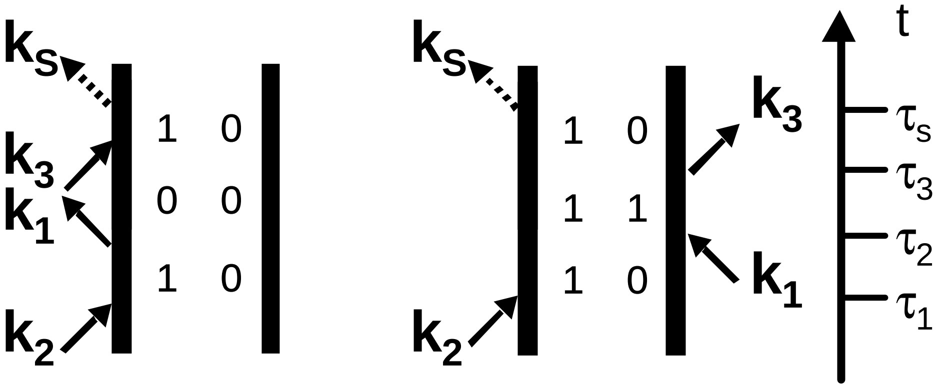

"non-rephasing" → virtual echo

} $t-t_3=t'$ $\qquad$ $e^{-i\omega_{10}t'-t'/T_2}$

} $t_2=\tau_{31}=T$ $\qquad$ e^{-T/T_1}

} $t_1=\tau_{21}=\tau$ $\qquad$ $e^{-i\omega_{10}\tau-\tau/T_2}$

Bloch Limit: 3PE Experiment

A $\langle \delta\omega(t)\delta\omega(0)\rangle = \delta(t)/T_2$ $I^{2PE}(t',\tau) \propto \exp(-2\tau/T_2 - 2T/T_1 - 2t'/T_2)$ $I^{2PE}(\tau) \propto \exp(-2\tau/T_2 - 2T/T_1)$

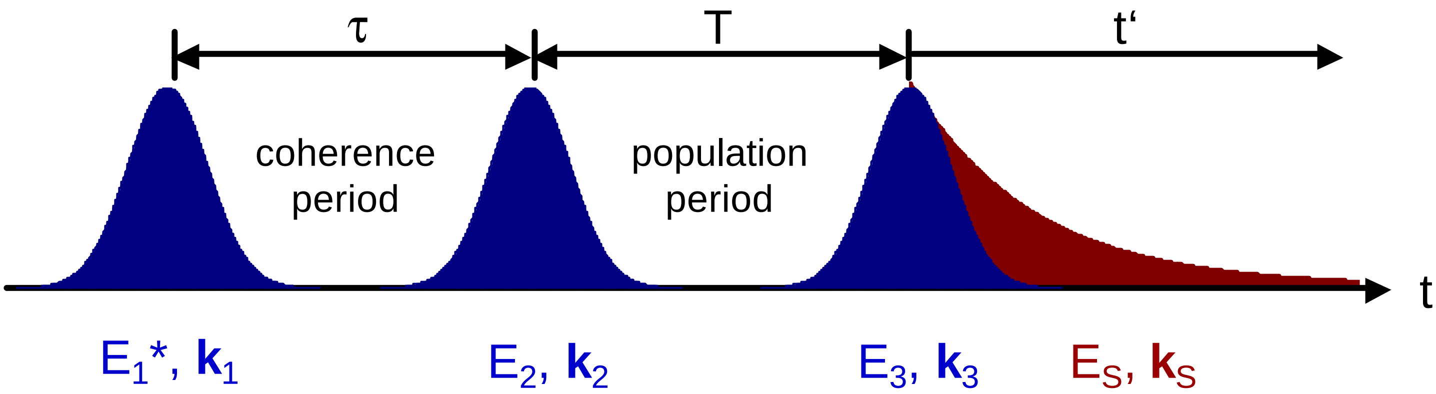

B $\langle \delta\omega(t)\delta\omega(0)\rangle = \delta(t)/T_2 + (\Delta_{ih})^2$ $I^{2PE}(t',\tau) \propto \exp(-2\tau/T_2 - 2T/T_1 - 2t'/T_2 - (\Delta_{ih})^2 (t'-\tau)^2)$

$I^{2PE}(\tau) \propto \exp(-4\tau/T_2 - 2T/T_1)$

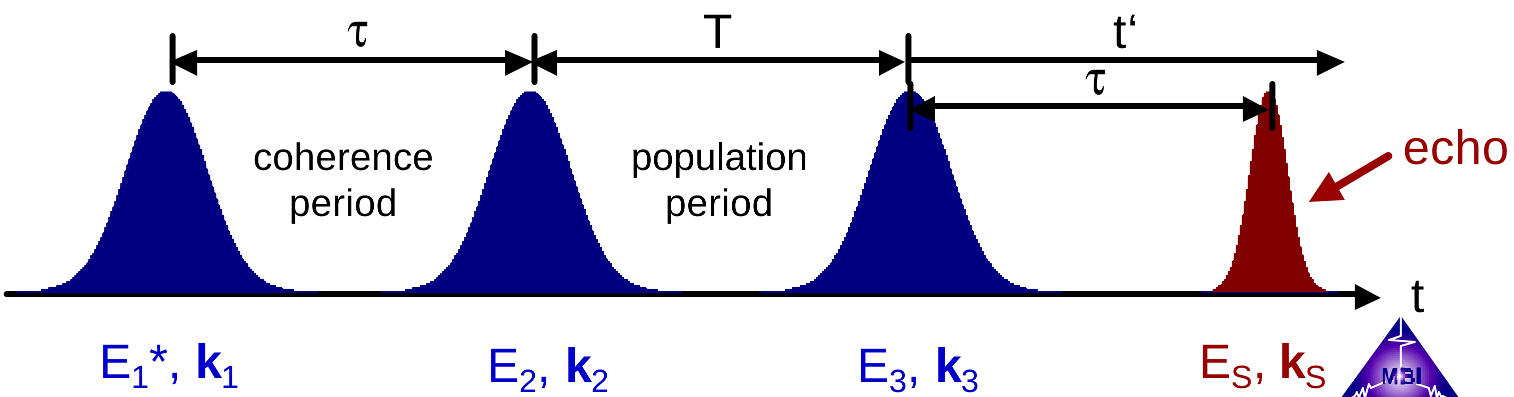

Frequency Gratings in 3PE Experiments

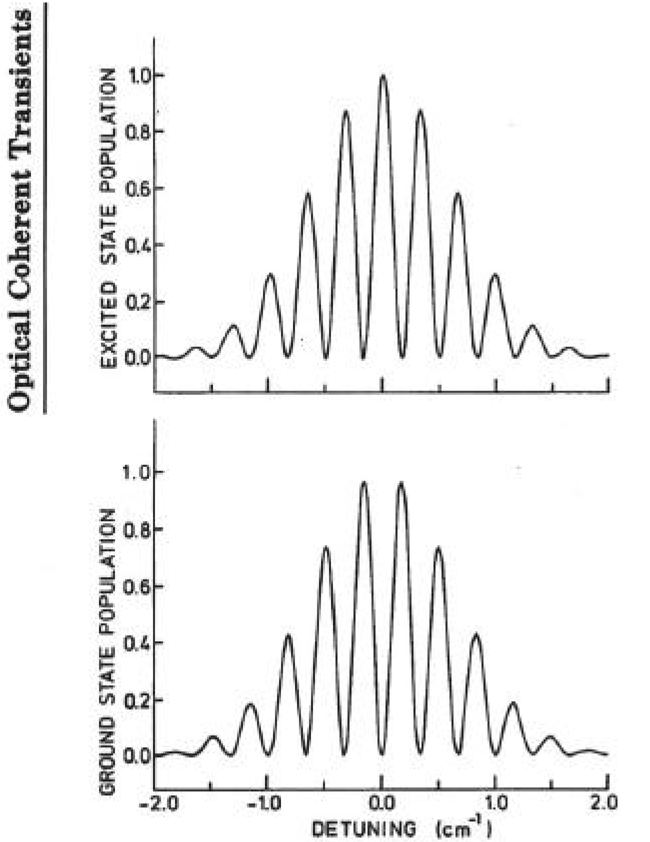

Fig. 3. Modulation of the population in states |1⟩ and |2⟩ after application of two resonant $\pi/2$ pulses separated by 100 psec. The horizontal axis gives the detuning from the line center. It does *not* indicate the absolute energy in either the ground or the excited state. The envelope of the modulation represents a line width of 1.5 cm^{-1}. The phase of the modulation was chosen to be zero.

- After interaction with field $E_1^*(\mathbf{k}_1)$, a coherence period, and a field interaction $E_2(\mathbf{k}_2)$, one has transiently generated frequency gratings in ground and excited states
- Modulation depth is given by nutation angle ($\pi/2$ or less)
- Frequency period is given by inverse of delay time between interactions $E_1^*(\mathbf{k}_1)$ and $E_2(\mathbf{k}_2)$.

K. Duppen and D.A. Wiersma,
J.Opt. Soc. Am. B **3**, 614 (1986)

3PE: Population Relaxation & Spectral Diffusion

After 2 interactions: frequency grating in ground & excited states

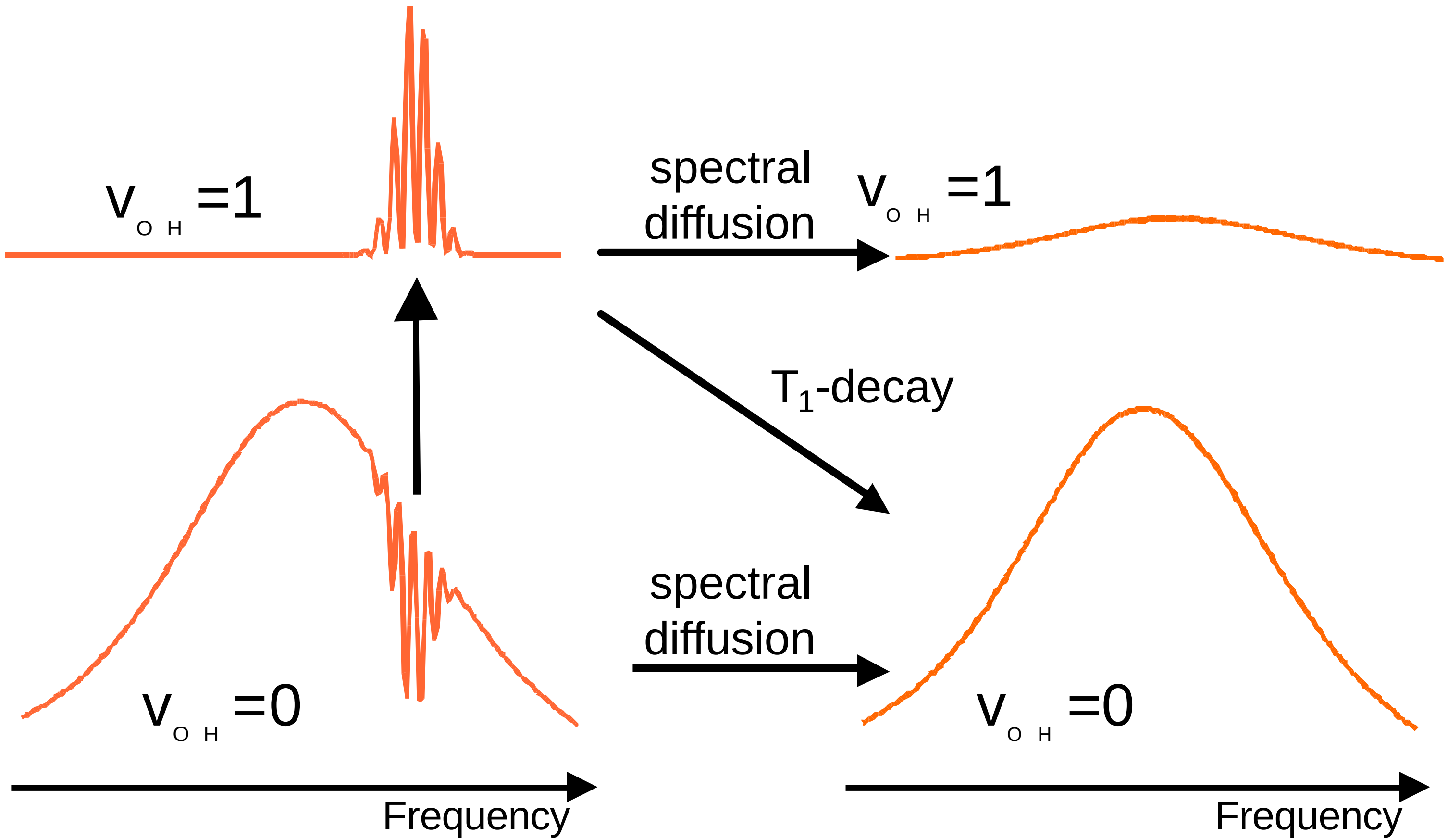

Echo Peak Shift Measurement

Echo Peak Shift: $\tau_{max}(T)$

Determine T-dependence of echo peak shift, given by $\tau_{max}(T)$ where $\partial S_{3PE}/\partial\tau = 0$

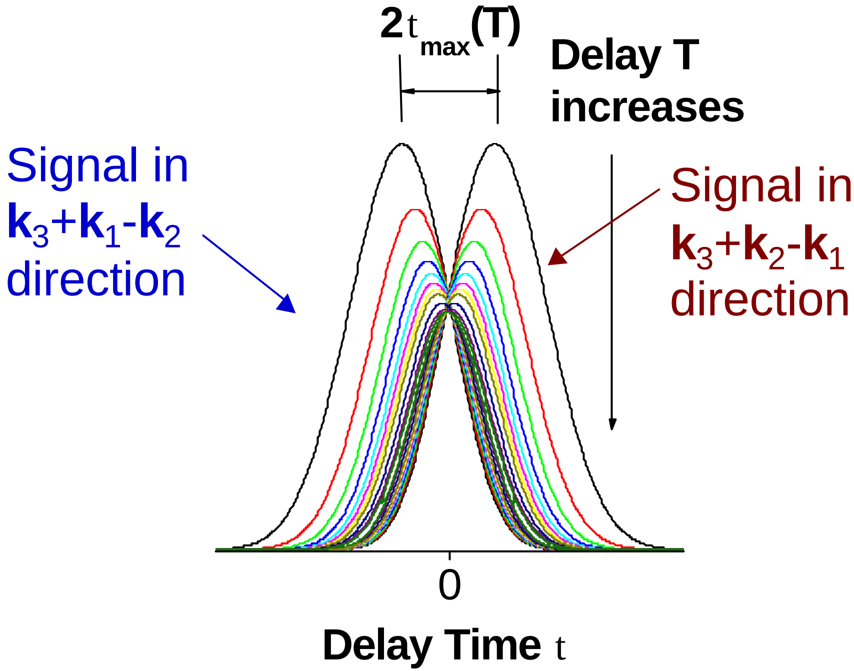

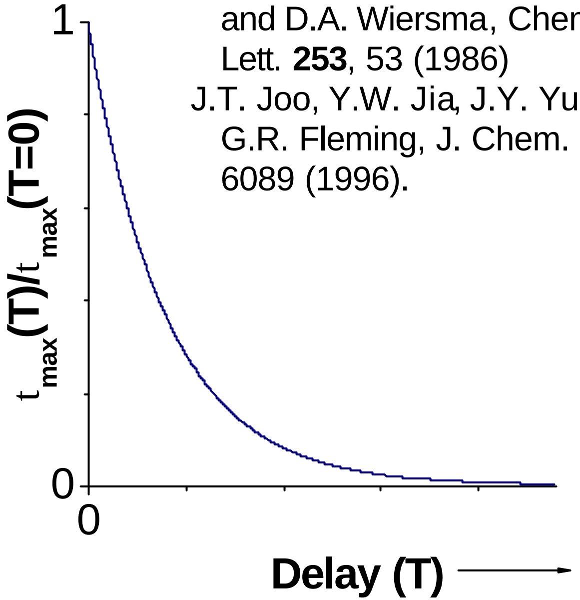

W.P.de Boeij, M.S. Pscheninichnikov and D.A. Wiersma, Chem. Phys. Lett. **253**, 53 (1986)

J.T. Joo, Y.W. Jia, J.Y. Yu, M.J. Lang, G.R. Fleming, J. Chem. Phys. **104**, 6089 (1996).

- Echo peak shift indicates inhomogeneity
- Decay of peak shift = decay of inhomogeneity
- Echo peak shift decay mimics frequency fluctuation correlation function for 2-level systems

Frequency-Dependent Echo Peak Shift of HOD/D_2O

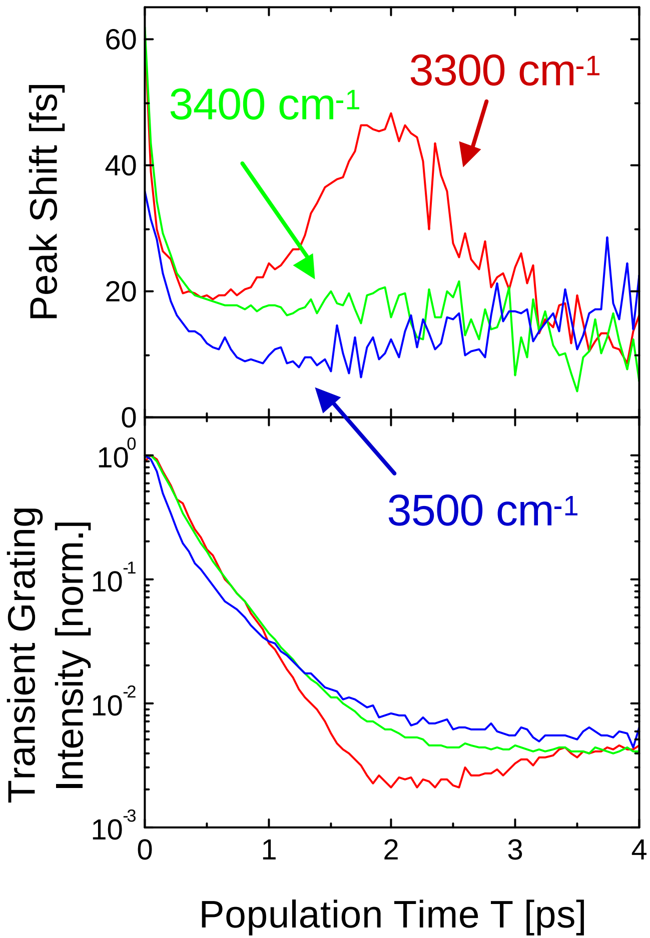

- Transient Grating does not decay further for T > 2 ps
- Peak shift has long ps-component
- Peak shift at 3300 cm^{-1} rises again until T = 2 ps and then decays again

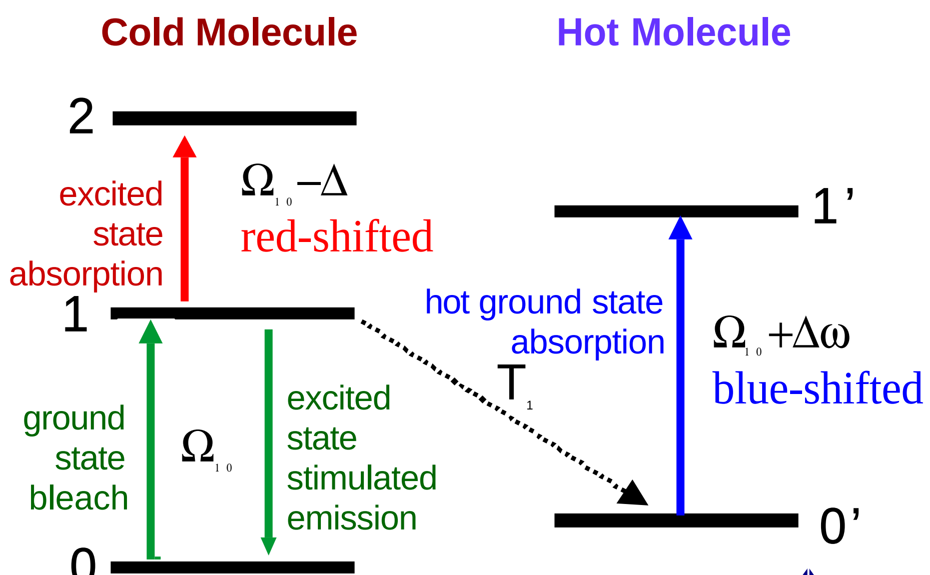

J. Stenger *et al*., J. Phys. Chem. A **106**, 2341 (2002)

Double-Sided Feynman Diagrams for 5-Level System

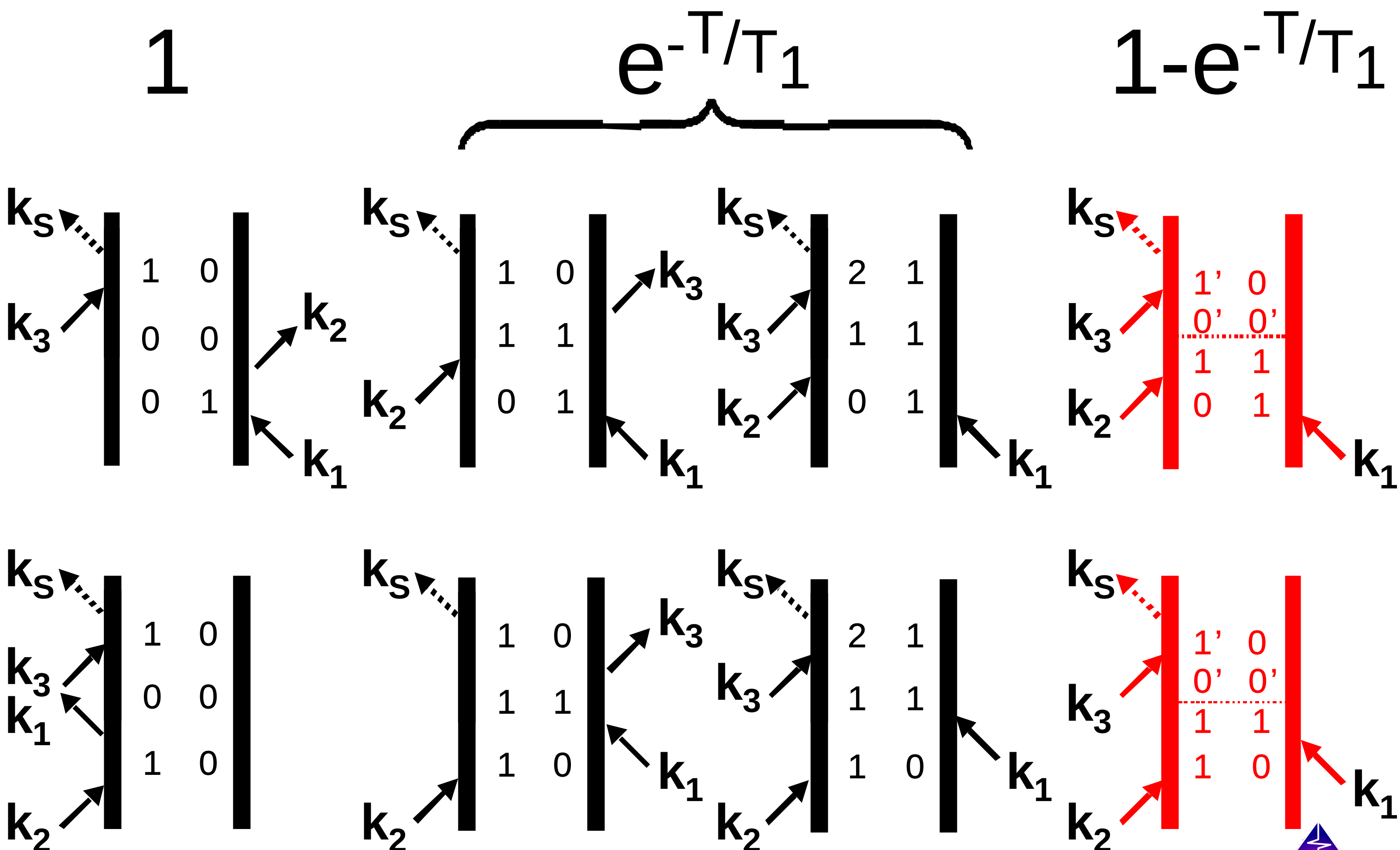

Calculations: 3-Level System – Kubo Model

Phase memory washed out by T_1-decay: $v_{OH}=1$ decays back to $v_{OH}=0$

$$\langle\delta\omega(t)\delta\omega(0)\rangle = \delta(t)/T_2 + \Delta_1^2\exp(-t/\tau_{c1}) + \Delta_2^2\exp(-t/\tau_{c2})$$

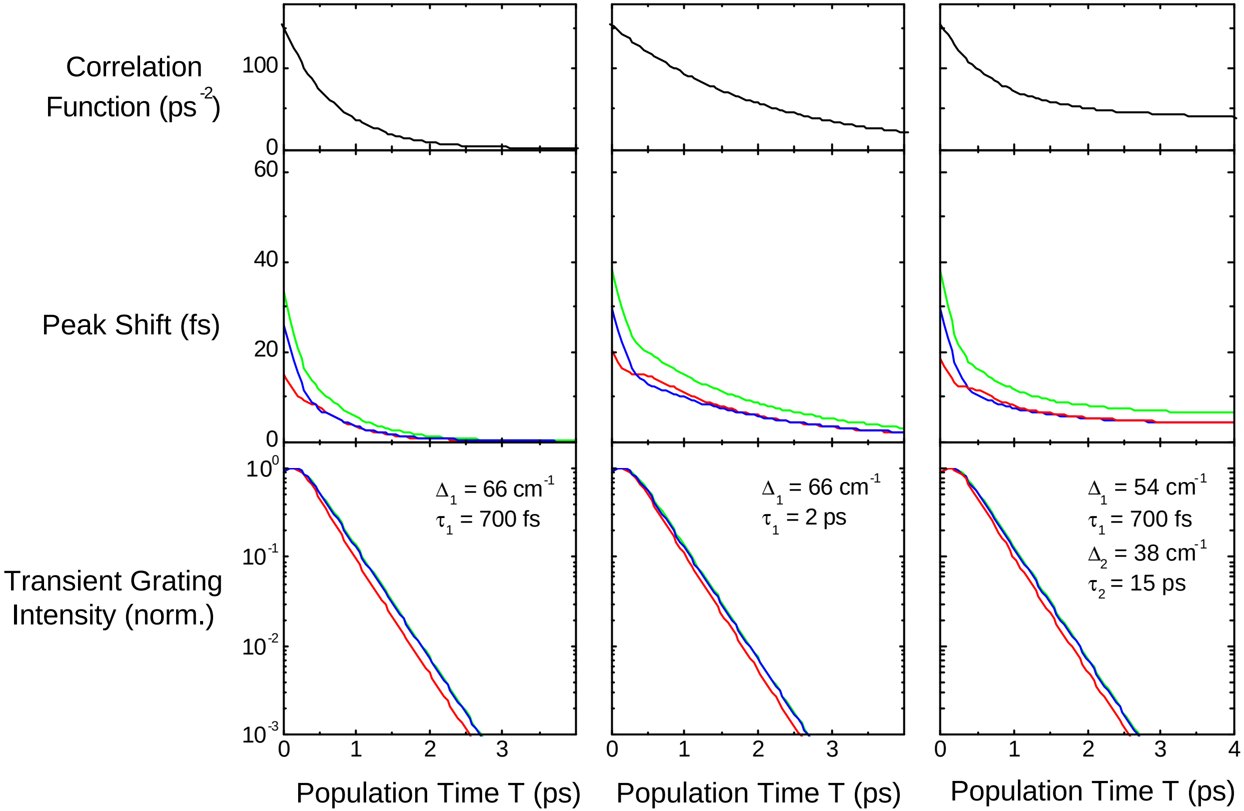

J. Stenger *et al.*, J. Phys. Chem. A **106**, 2341 (2002)

Correlated vs. Uncorrelated T_1-Dynamics

- Three Pulse Photon Echo: phase memory stored in frequency grating
- Frequency grating remains or disappears during population decay of $v_{OH}=1$

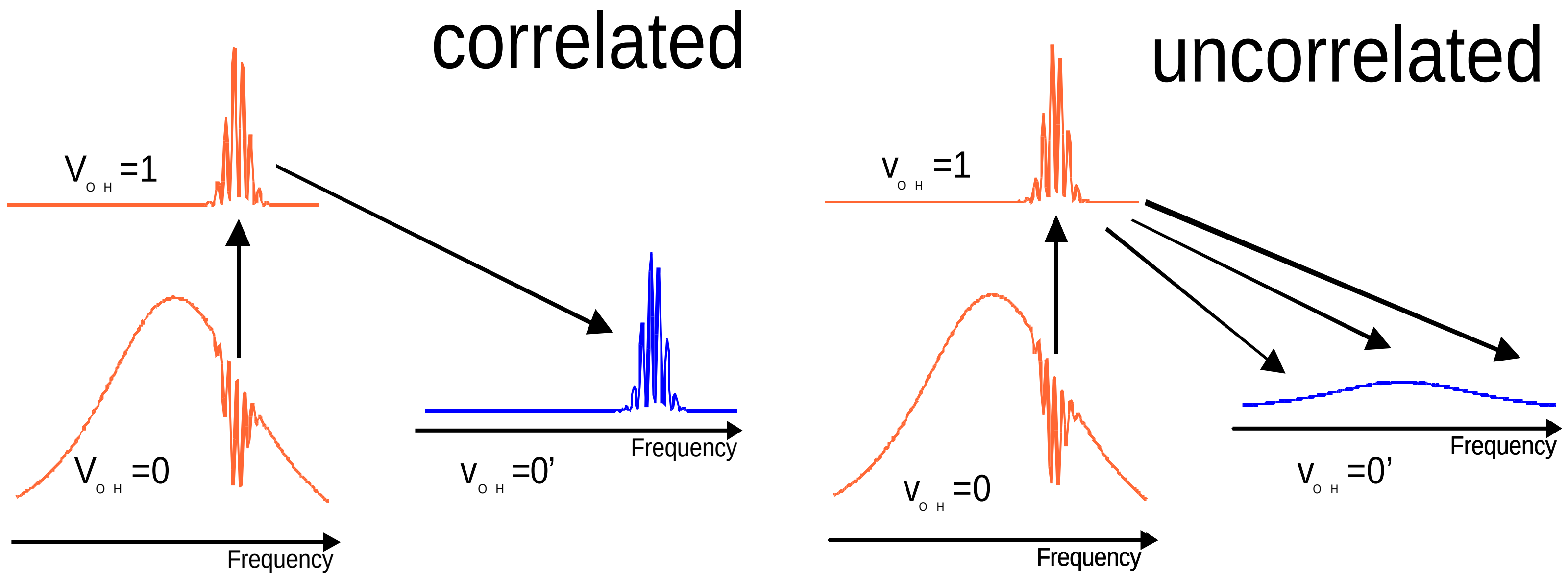

Calculations: 5-Level System — Bloch Model

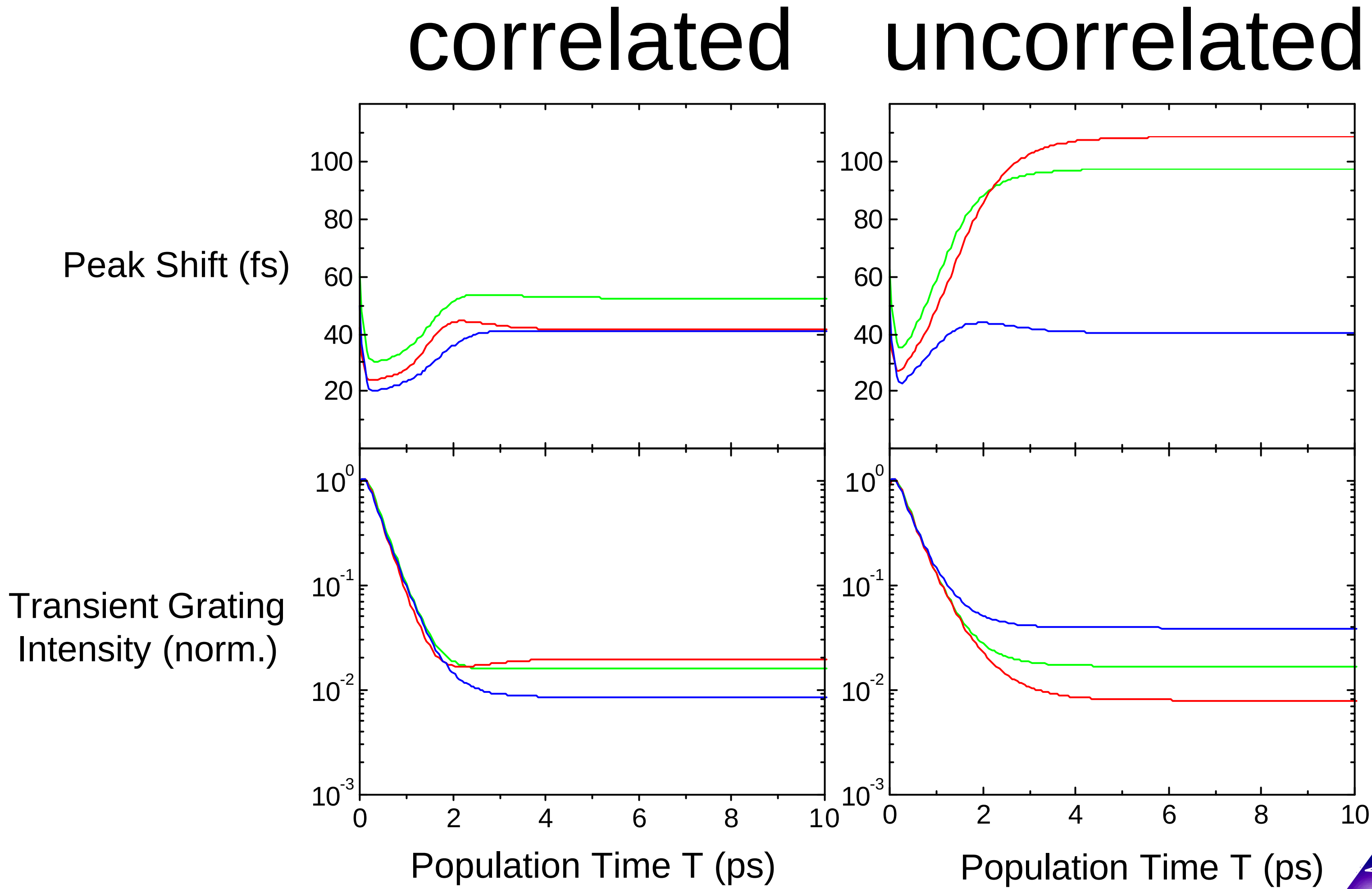

J. Stenger *et al.*, J. Phys. Chem. A **106**, 2341 (2002)

Calculations: 5-Level System – Kubo Model I

Correlated dynamics: Phase memory not affected by T_1-decay

$$\langle \delta\omega(t)\delta\omega(0) \rangle = \delta(t)/T_2 + \Delta_1^2 \exp(-t/\tau_{c1}) + \Delta_2^2 \exp(-t/\tau_{c2})$$

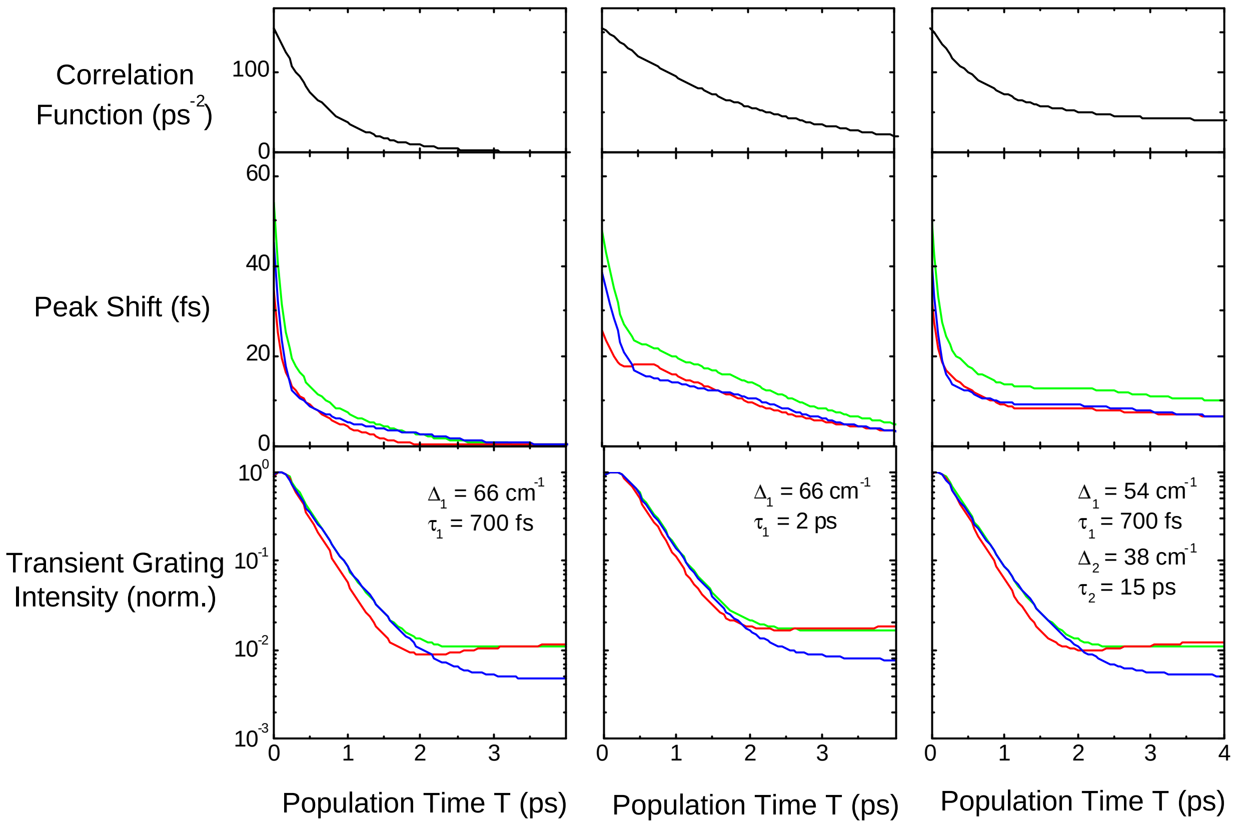

J. Stenger *et al.*, J. Phys. Chem. A **106**, 2341 (2002)

Calculations: 5-Level System – Kubo Model II

Uncorrelated dynamics: Phase memory washed out by T_1-decay

$$\langle\delta\omega(t)\delta\omega(0)\rangle = \delta(t)/T_2 + \Delta_1^2\exp(-t/\tau_{c1}) + \Delta_2^2\exp(-t/\tau_{c2})$$

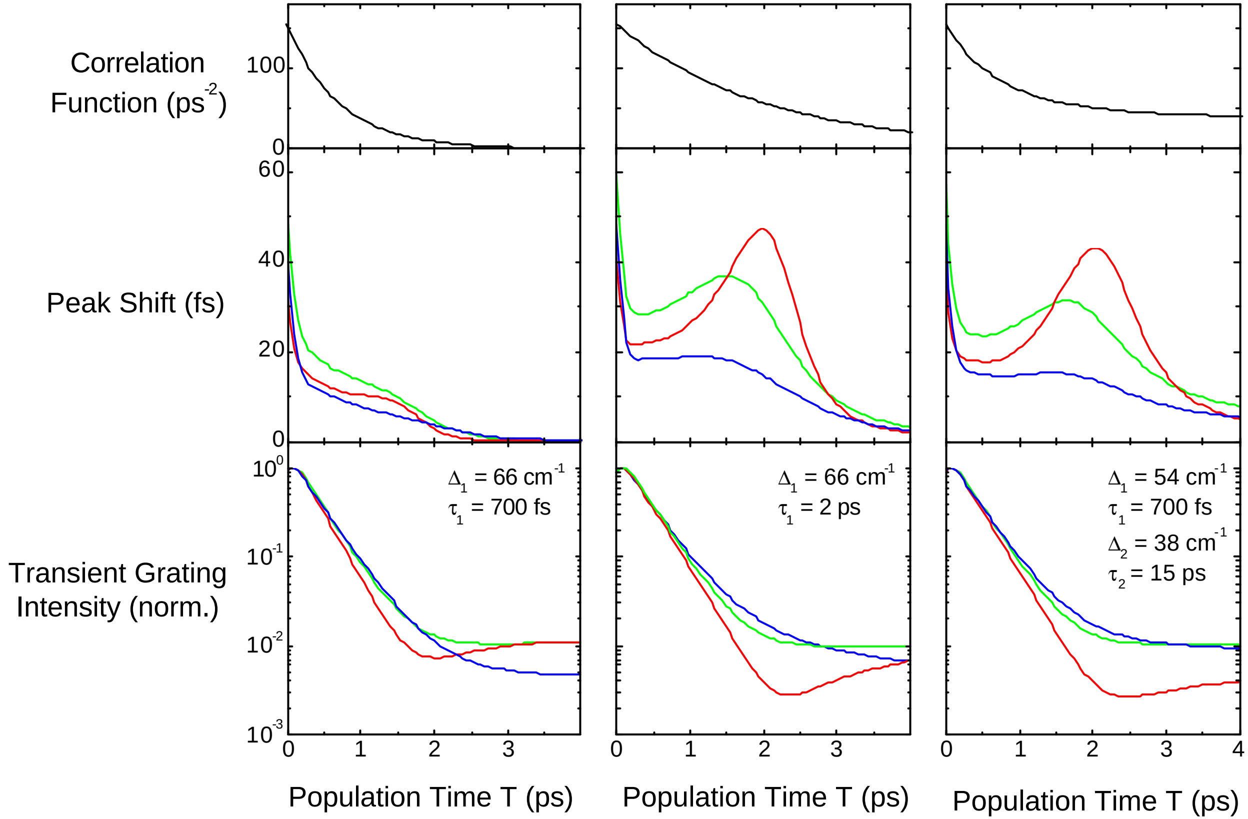

J. Stenger *et al.*, J. Phys. Chem. A **106**, 2341 (2002)

Calculated Four-Wave Mixing Signals: Kubo Model

$$\langle \delta\omega(t)\delta\omega(0) \rangle = \delta(t)/T_2 + \Delta_1^2 \exp(-t/\tau_{c1}) + \Delta_2^2 \exp(-t/\tau_{c2})$$

J. Stenger *et al*.,
J. Phys. Chem. A,
106, 2341 (2002)

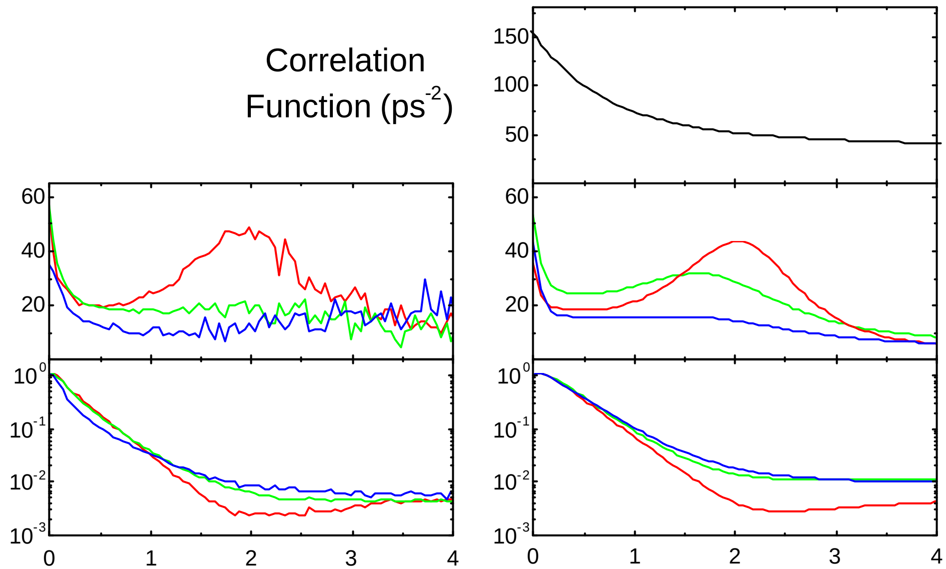

3rd column: best calculated result with

T_2 = 90 fs

Δ_1 = 54 cm^{-1}
τ_{c1} = 700 fs

Δ_2 = 38 cm^{-1}
τ_{c2} = 15 ps

Cf. MD simulations: response at multitude of time scales!
See e.g. Diraison et al. [CPL **258**, 348 (1996)]: 50 fs and 800 fs components.
See also: Marti et al. [JCP **105**, 639 (1996)]; Luzar and Chandler [Nature **379**, 55 (1996)].

What Else?

PRINCIPLES OF NONLINEAR OPTICAL SPECTROSCOPY

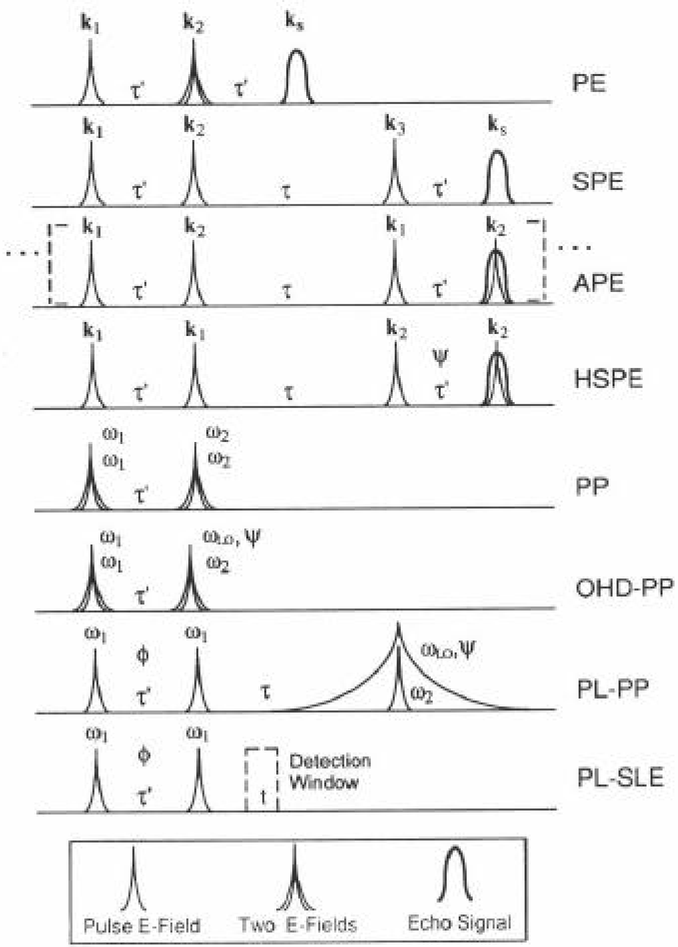

FIG. 10.7 Pulse sequences for the various $P^{(3)}$ techniques. PE, photon echo; SPE, stimulated photon echo; APE, accumulated photon echo; HSPE, heterodyne-detected stimulated photon echo; PP, pump-probe; OHD-PP, optical heterodyne-detected pump-probe; PL-PP, phase-locked pump-probe; PL-SLE, phase-locked spontaneous light emission. The pump-probe techniques will be surveyed in Chapter 11. In APE and HSPE, the fourth pulse coincides spatially and temporally with the echo signal. The phase relations between the two consecutive pulses are adjusted as ϕ and ψ in HSPE, PL-PP, and PL-SLE. On the other hand, the optical phase of the local oscillator (of frequency, ω_{LO}) is described as ψ in OHD-PP and PL-PP. [From M. Cho, N. F. Scherer, G. R. Fleming, and S. Mukamel, "Photon echoes and related four wave mixing spectroscopies using phase-locked pulses," *J. Chem. Phys.* **96**, 5618 (1992).]

Essential Reading on Photon Echo Spectroscopy

- Books, reviews

S. Mukamel, *Principles of Nonlinear Optical Spectroscopy* (Oxford University Press, Oxford, 1995).

L. Allen and J. H. Eberly, *Optical Resonance and Two-Level Atoms* (Dover, New York, 1975).

- Photon echoes on atoms in the gas phase

N. A. Kunrit, I. D. Abella and S. R. Hartmann, Phys. Rev. Lett. **13**, 567 (1964).

- Optical photon echo on molecules in the condensed phase

T. J. Aartsma and D. A. Wiersma, Phys. Rev. Lett. **36**, 1360 (1976).
W.H. Hesselink and D.A. Wiersma, Phys. Rev. Lett. **43**, 1991 (1979).
P. C. Becker, H. L. Fragnito, J.-Y. Bigot, C. H. Brito-Cruz, R. L. Fork and C. V. Shank, Phys. Rev. Lett. **63**, 505 (1989).
E. T. J. Nibbering, K. Duppen and D. A. Wiersma, Phys. Rev. Lett. **66**, 2464 (1991).
M. H. Cho and G. R. Fleming, Annu. Rev. Phys. Chem. **47**, 109 (1996).
W. P. de Boeij, M. S. Pshenichnikov and D. A. Wiersma, Annu. Rev. Phys. Chem. **49**, 99 (1998).

- Vibrational photon echo

A. Tokmakoff and M. D. Fayer, Acc. Chem. Res. **20**, 437 (1995).
P. Hamm and R. M. Hochstrasser, in *Ultrafast Infrared and Raman Spectroscopy*, M. D. Fayer, Ed., (Marcel Dekker, New York, 2001), pp. 273-348.
M. C. Asplund, M. T. Zanni, R. M. Hochstrasser, Proc. Nat. Acad. Sci. U.S.A. **97**, 8219 (2000).
J. Stenger, D. Madsen, P. Hamm, E. T. J. Nibbering and T. Elsaesser, Phys. Rev. Lett. **87**, 027401 (2001); J. Phys. Chem. A **106**, 2341 (2002).